Thermal characterization of magnesium containing ionomer glasses

ELENI MARIA KARTELIA
Supervisor: Dr. A. Stamboulis

Thesis submitted for the degree of
MRes Biomaterials

University of Birmingham

School of Engineering

Department of Metallurgy and Materials

September, 2010

UNIVERSITY OF BIRMINGHAM

University of Birmingham Research Archive

e-theses repository

ACKNOWLEDGMENTS

I would like to thank my supervisor Dr. A. Stamboulis for her help and encouragement during my project. Without her support, I feel that I would not have been able to complete this work.

I would also like to express my gratitude to Dr. D. Holland at University of Warwick for her helping on DSC measurements. Many thanks are given to academic staff and technicians of the School of Metallurgy and Materials.

I would like to thank sincerely the Phd students Praveen Ramakrishnan, Georgina Kaklamani, Siqi Zhang and Mitra Kashani for their significant help through my experimental work.

Last but not least, I would like to thank my family for their support and understanding. Special thanks to Thanos Papaioannou.

TABLE CAPTIONS

CHAPTER 2: MATERIALS AND METHODS

Table 2.1.2:   Composition of Mg substituted alumino-silicate glasses.

CHAPTER 3: RESULTS

Table 3.1:   DSC analysis data for all Mg containing glasses (particle size >45μm) measured at a heating rate of 10°C/min.

Table 3.2:   Analysis of XRD patterns of different Mg containing glass-ceramics.

Table 3.3:   Comparison of the crystal size and type of Ca fluorapatite $(Ca_5(PO_4)_3F)$, wagnerite $(Mg_2(PO_4)F)$ and mullite $(Al_6Si_2O_{13})$ phase formed in glass-ceramics with different Mg content.

Table 3.4:   Optimum nucleation temperature and activation energies in Mg containing glasses for FAP crystallisation determined by the Marotta and Kissinger method (Matusita)

FIGURE CAPTIONS

CHAPTER 1: LITERATURE REVIEW

Figure 1.1:   Setting reaction of a glass ionomer cement [25].

Figure 1.2:   An example of the basic structure of tetrahedral units in silicate glasses[44].

Figure 1.3:   The figure indicates the fluorapatite crystal growth which is inhibited by the size of the droplet. The droplet phase size is equivalent to the fluorapatite crystal size. Reaching the transition temperature of the second phase stimulates the fluorapatite crystal to exceed the droplet phase boundaries [39].

Figure 1.4:   SEM of a fracture surface showing elongated apatite crystals with a high lenth to diameter aspect ratio [16].

CHAPTER 3: RESULTS

Figure 3.1:   Density of Mg containing glasses.

Figure 3.2:   Oxygen Density of Mg containing glasses.

Figure 3.3:   FTIR spectra of all Mg substituted glasses.

Figure 3.4:   DSC trace of calcium containing glass LG26 with particle size >45μm measured at a heating rate of 10°C/min.

Figure 3.5:   DSC traces of all Mg containing glasses ((a) LG26(25%)Mg, (b) LG26(50%)Mg, (c) LG26(75%)Mg, (d) LG26(100%)Mg) with particle size ranging from 3mm to 45μm-100 μm measured at a heating rate of 10°C/min.

Figure 3.6:   Density of Mg containing glass ceramics.

Figure 3.7:   X-ray powder diffraction patterns of heat treated Mg glass-ceramics. F = Fluorapatite, M = Mullite, W = Wagnerite.

ABBREVIATIONS

A	Apatite
APS	Amorphous Phase Separation
AW	Atomic Weight
BO	Bridging Oxygens
Ca-FAP	Calcium Fluorapatite
DSC	Differential Scanning Calorimetry
Ea	Activation Energy
Ca-FAP	Fluorapatite
FTIR	Fourier Transform Infrared Spectroscopy
GICs	Glass Ionomer Cements
HA	Hydroxyapatite
M	Mullite
MAS-NMR	Magic Angle Spinning Nuclear Magnetic Resonance
NBO	Non-Bridging Oxygens
rA/rO	Ratio of the ionic radii of the atom A and the atom O
SEM	Scanning Electron Microscopy
Tg	Glass Transition Temperature
Tn	Optimum Nucleation Temperature
Tp1	First Crystallisation Peak Temperature
Tp'1	The crystallisation peak temperature occurring after nucleation hold
Tp2	Second Crystallisation Peak Temperature
W	Wagnerite
XRD	X-ray Diffraction

CONTENTS

ABSTRACT

Ionomer glasses are one of the components to produce glass ionomer cements or glass polyalkenoate cements, a popular type of white dental fillings. A typical glass composition for this application is 20-36% wt.% SiO_2, 15-40% Al_2O_3, 0-35% CaO, 0-10% $AlPO_4$, 0-40% CaF_2, 0-5% Na_3AlF_6 and 0-6% AlF_3. These glasses can be made by mixing the appropriate oxides followed by fusion of ingredients in the temperature range of 1200 ˚C to 1590 ˚C.

The glass composition used in this study is $4.5SiO_2$-$3Al_2O_3$-$1.5P_2O_5$-$3CaO$-$2CaF_2$. A series of new glasses were produced by Mg substitutions for Ca. Magnesium replaced calcium, by 25 (LG26 25%Mg), 50 (LG26 50%Mg), 75 (LG26 75%Mg) and 100 molar % (LG26 100%Mg). The new glasses were characterised by Helium Pycnometer, FTIR, DSC and XRD. The optimum nucleation temperatures and activation energies were calculated by DSC, the crystal size was measured using the Sherrer equation from the XRD patterns and finally the chemical structure was analysed by FTIR. The glass density and the oxygen density were calculated in order to understand how magnesium substitutions can affect the glass network.

In this study was showed that the density of glasses and glass ceramics decreased whereas the oxygen density increased slightly with Mg substitution. Furthermore in FTIR spectra there are four absorption regions of Mg containing aluminosilicate glasses which were associated with stretching and bending vibrations. In FTIR was also observed some shift towards higher wavenumbers with Mg substitution. On the other hand, DSC analysis showed that the glass transition temperature (Tg), Tp1 and

Tp2 did not undergo significant changes with Mg substitution comparing all Mg substituted glasses but a significant change was observed between the Tp1 and Tp2 values of LG26 and Mg substituted glasses. A decrease in optimum nucleation temperature (Tn) with Mg substitution in all Mg substituted glasses except of LG26(100%)Mg was also observed. The LG26(100%)Mg glass did not exhibit an optimum nucleation temperature indicating that the glass undergoes spontaneous crystallisation. Furthermore, XRD analysis showed that the substitution of Mg for Ca resulted in the formation of Wagnerite (Mg_2PO_4F), Ca-FAP and Mullite ($Al_6Si_2O_{13}$) in the case of LG26(25%)Mg and LG26(50%)Mg containing glass ceramics and Wagnerite (Mg_2PO_4F) and Mullite ($Al_6Si_2O_{13}$) in the case of LG26(75%)Mg and LG26(100%)Mg glass ceramics. The crystal size and the activation energy of Ca-FAP/Wagnerite were calculated. The activation energy increased for all glass compositions with the exception of LG26(75%)Mg.

CHAPTER 1

LITERATURE REVIEW

1.1 Introduction

Ionomer glasses are used to form glass ionomer cements and play an important part to the structural features and the properties of glass ionomer cements which affect their application range. Glass ionomer cements are adhesive to the tooth structure, translucent and biocompatible [1]. Wilson and Kent developed the first glass-ionomer cement in the Laboratory of the Government Chemist in UK formed by an acid-base reaction between basic fluoro-alumino-silicate glass and a polyacrylic acid in the presence of water. The glass ionomer cements that are available in the market today show much improved mechanical properties compared to the ones used in the past [2-8].

Dental cements are made out of an alumino silicate glass type containing Ca and fluoride ions. These glasses can be made by oxide mixing followed by fusion of ingredients in the temperature range of 1200°C to 1590°C which is composition dependant. A typical composition is 20-36% SiO_2 wt.%, 15-40% Al_2O_3, 0-35% CaO, 0-10% $AlPO_4$, 0-40% CaF_2, 0-5% Na_3AlF_6 and 0-6% AlF_3. Ions are leaching out from the glass while the cement is set as a result of the glass surface acid base reaction with the polymeric acid, resulting in cation release and consequently cross-linking of the polymer chains (Figure 1.1) [1, 9-11].

Setting Reaction
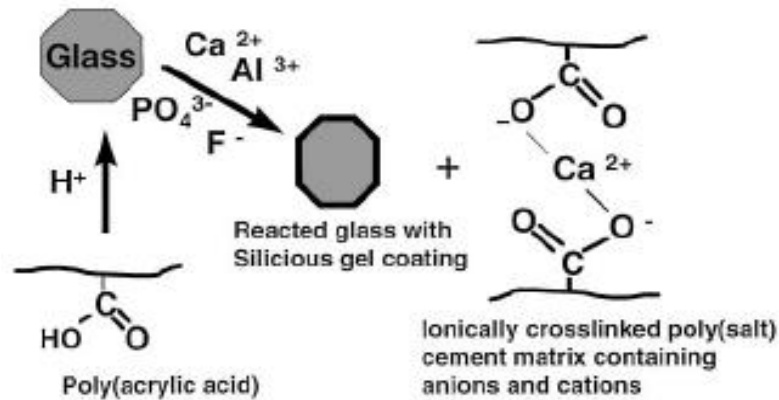
Figure 1.1: Setting reaction of a glass ionomer cement [25]

It is important to note, that the mechanical properties of cements are affected by the silicon to aluminium ratio as well as the fluorine in the glass structure. The influence of the silicon to aluminium ratio can be reduced by the high phosphorus content of glasses since phosphorus locally charge balances the four-fold coordinated aluminium ions in the glass network reducing the number of Al-O-Si bonds available for acid hydrolysis and therefore delaying the setting reaction. It is generally accepted that low phosphorus containing ionomer glasses are more reactive than high phosphorus containing ionomer glasses. Aluminium as an intermediate oxide acts as network former entering the silica network and conferring a negative charge in the network making it susceptible to the acid hydrogen ions attack [12]. Lowenstein's theory states that if two tetrahedral units are linked by one oxygen bridge, the centre of only one of them can be occupied by a tetrahedral aluminium. Occupation by silicon, or another small ion of electrovalence of four or more, e.g. phosphorus must occur in the other centre [45]. If aluminium is the second centre it must be at a higher coordination state

e.g. five or six coordination. Apart from the composition, other factors were taken into account for the use of this glass:

- Each silicon has at least one NBO (non bridging oxygen) as part of its composition

- The amount of fluorine in the glass should be less than that of aluminium in order to minimize the formation of volatile SiF_4 during melting [46]. The second criterion can be explained on the basis that one Si^{4+} cation can be replaced easier with NBOs or O^{2-} anions than with a non-bridging fluorine or F^- anion and that an Al^{3+} ion should bond to F^- anions preventing the formation of Si-F bonds in the glass network. This explanation is supported by a trimethylsilylation analysis reported in a previous study of $2SiO_2$-Al_2O_3-CaO-CaF_2 glass that showed absence of Si-F bonds in the glass structure [47].

On the other hand, fluorine plays an important role in the properties of ionomer glasses and glass ionomer cements. The presence of fluorine decreases the glass transition temperature, the melting temperature and the viscosity of ionomer glasses as well as the refractive index of the glass and generally disrupts the glass network facilitating the acid attack and is released directly by the ionomer glass, during cement formation. Furthermore, the presence of fluoride (CaF_2) enhances the compressive strength (reaching values even above 200 MPa) and Young's modulus but does not seem to significantly influence the fracture toughness of glass ionomer cements, that is strongly dependent on the polyacid molecular weight [5, 7, 12, 13, 15-18].

Glasses with appropriate compositions can be heat-treated and thus undergo controlled crystallisation to form glass-ceramics, in which the main crystalline phase

is apatite, similar to the apatite phase in bones and teeth [15]. One of the most important glass ceramics are apatite-mullite glass ceramics and are the result of the crystallisation of the following general glass composition $4.5SiO_2-3Al_2O_3-1.5P_2O_5-(5-x)CaO-xCaF_2$.

1.2 Composition and Structure of Ionomer glasses

As was already described, the main components of ionomer glasses are 20-36% SiO_2 wt.%, 15-40% Al_2O_3, 0-35% CaO, 0-10% $AlPO_4$, 0-40% CaF_2, 0-5% Na_3AlF_6 and 0-6% AlF_3. The composition of glasses affects the rate of ion release. There are three different types of glasses that have been used in the glass ionomer cements. These are aluminosilicate, aluminoborate and zinc silicate glasses:

1) Alumino silicate glasses, that have been mainly studied by Wilson and co-workers and are based on the systems SiO_2 - Al_2O_3 – CaO or SiO_2 - Al_2O_3 - CaF_2 [11]. Low amounts of alkali and alkali oxides (e.g. MgO and CaO) are present in the commercial glasses of this type. The glasses exhibit high elastic modulus and a high chemical corrosion resistance. The vast population of low-alkali aluminosilicates can be transformed into glass ceramics readily and have been used in various applications including cookware and dental implants [19]. These glass ceramics show good chemical durability, tolerance in higher temperatures and superior strength properties. Despite the fact that aluminosilicate glasses have been studied for a long time their structure and chemical bonding is not completely understood [20, 21].

2) Alumino borate glasses studied by Combe et al are based mainly on the system $Al_2O_3 - B_2O_3 - ZnO - ZnF_2$ [22]. This type of glasses referred to as alumino borate glasses are fairly important because of their ability to be hydrolysed in aqueous environments. Yet after research, the alumino borate glasses were found to have relatively poor chemical durability. The corresponded cements of alumino borate glasses exhibit a limited compressive strength compared to alumino silicate glass-formed ionomer cements. This makes the alumino borate glasses unsuitable for the formation of cement [11].

3) Zinc silicate glasses based on the system $CaO - ZnO - SiO_2$ or $Al_2O_3 - ZnO - SiO_2$ have been investigated by Hill et al [43]. This type of ionomer glasses gives rise to high strength glass ionomer cement. The glass reactivity and the ability to form cement are determined by the network connectivity depending on the role of zinc in the glass network whether this is a network modifier or an intermediate oxide. The cement formed though, seemed to be unsuitable for dental use since it is hydrolysed leading to degradation together with its general weakness. Furthermore, zinc is important for the function of the immune system and has been recognised as an antibacterial agent. Hence Zn-glass polyalkenoate cements can be used as hard tissue replacement materials [11, 14].

Modification of the glass powder component using various methods occurs readily in order to improve the glass ionomer strength. These methods include changing the composition (e.g. the fluoride and sodium content and the aluminium : silicate ratio), addition of bioactive components (e.g. certain glasses and hydroxyapatite) and

reinforcing by incorporating metal particles (e.g. silver-tin alloy, gold, platinum, palladium, stainless steel or fibres such as carbon steel or glass) [23].

Goldschmidt's radius ratio criterion and Zachariasen's random network theory are the two main theories on glass formation, both of which have been thoroughly investigated and for both of which a great deal of information is known. Concerning Goldschmidt, in the early 1920's he proposed a rule for the formation of a glass based on the knowledge about glass formation oxides, such as SiO_2. He stated that if an oxide is expressed as A_mO_n, the ratio of the ionic radii of the atom A and the atom O, rA/rO, needs to be between 0.2 and 0.4 for glass formation. This implies the tetrahedral coordination of the glass forming cation [44]. Zachariasen on the other hand defined a glass as "a substance that can form an extended three-dimensional network that is lacking periodicity with energy content comparable with that of the corresponding crystal network" and summarized basic rules (1, 2, 3, 4) for glass formation in simple oxides as well as modified rules (5, 6, 7) for complex glasses respectively, which have been developed during extensive usage for formulating a continuous 3-dimensional glass network. These rules are summarised below (Figure 1.2) [19]:

1. Each oxygen atom is linked to no more than two cations.

2. The oxygen coordination number of the network cation is small.

3. Oxygen polyhedra share only corners and not edges or faces.

4. At least three corners of each oxygen polyhedron must be shared in order to form a 3D network.

5. The sample must contain a high percentage of network cations which are surrounded by oxygen tetrahedral or triangles.

6. The tetrahedra or triangles share only corners with each other.

7. Some oxygens are linked only to two network cations and do not form further bonds with any other cation.
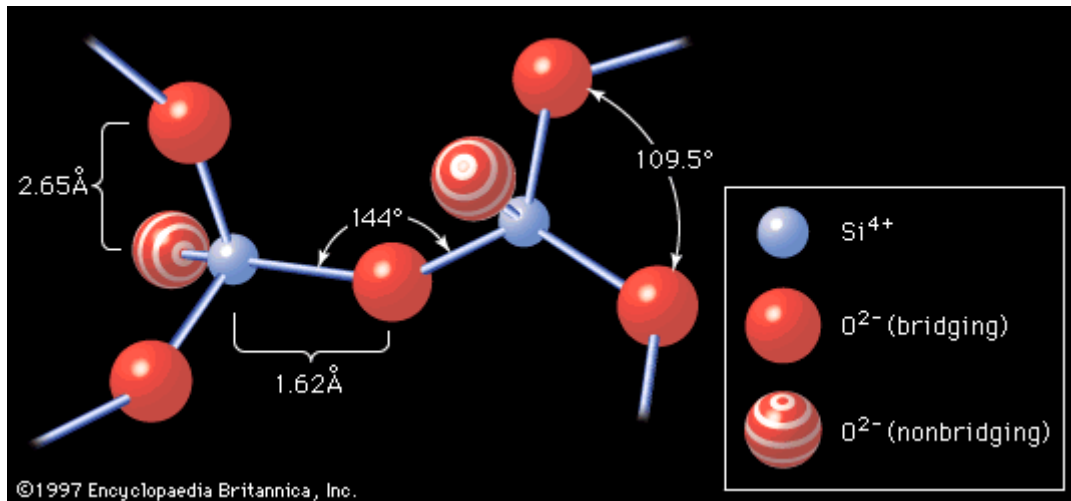
Figure 1.2: An example of the basic structure of tetrahedral units in silicate glasses [44].

The structural role of fluorine in ionomer glasses has been a main issue in research due to their broad use in the formation of glass polyalkenoate cements. The role of fluorine in the glass network and glass ionomer cements is summarised below [1, 7, 9, 11, 12, 28-32]:

1. Fluorine decreases the melting temperature and the viscosity of the ionomer glass as well as the refractive index of the glass.

2. Fluorine disrupts the glass network facilitating the acid attack during cement formation.

3. During cement formation, fluorine is released directly by the ionomer glass without the need to add other fluorine compounds leading to a lower refractive index. Hence, an improved translucency of the cement is adopted together with a

lower fusion temperature, improving the working characteristics of the cement paste.

4. The presence of fluorine does not influence the fracture toughness of glass ionomer cements.

5. Fluoride constantly being released is responsible for the inhibition of the formation of secondary caries.

6. Fluoride enhances the compressive strength (which is reaching values above 200 MPa) and Young's modulus of glass ionomer cements.

7. An increase in the fluorine content results in a significant reduction in the glass transition temperature. The reduction was attributed to the replacement of BOs by non bridging fluorines resulting in an overall reduction in the network connectivity. This consequently allows network motion at a lower temperature [33].

The use of calcium fluoro-alumino-silicate glasses for the formation of glass ionomer cements (GICs) which is in turn used for medical and dental applications (as luting cements, bases, anterior filling materials and increasingly as posterior filling materials and bone cements) has attracted the interest of scientists in the last 10 years. The above ionomer glass compositions have the ability of forming apatite and mullite crystal phases which are then used for apatite-mullite glass-ceramics formation. These ceramics have excellent osteo-integration and osteo-conduction properties when implanted in the body as has been reported by Freeman et al. [24].

As was already mentioned, the generic glass composition SiO_2-Al_2O_3-P_2O_5-CaO-CaF_2 determines the properties of glass ionomer cements (GICs). Particularly, the Al/Si

ratio influences the glass properties and the properties of the resulting glass-ionomer cements and glass-ceramics as derived after studies and scientific experiments. Yet, the influence of Al/Si can be reduced by the high phosphorous content of the glasses since phosphorus can locally charge balance four-fold coordinated aluminium ions in the glass network which as a result has reduced number of Al-O-Si bonds available for acid hydrolysis [25]. In simple phosphorus-free alumino-silicate-glasses, hydrolysis of Si-O-Al bonds occurs and a silica gel layer is formed around the remaining glass particles. During this process Al and Ca are released that can ionically cross link the polyacrylic acid chains to form a polysalt matrix.

On the other hand, when glasses have high phosphorus content or if they have undergone amorphous phase separation, a special type of hydrolysis occurs, known as the P-O bonds hydrolysis [26]. During the hydrolysis of amorphous phase separated glasses, the phosphate groups compete with carboxylate groups for aluminium and calcium ions resulting in the inhibition of the cross-linking reaction in the cement matrix. Moreover, glasses with high phosphorous content show a significant decrease in the compressive strength and Young's modulus of the cement.

In order to improve the glasses used in glass ionomer cement formation, extensive research has been taking place studying the behaviour of glasses undergoing amorphous phase separation. Cement improvement is highly important since it is involved in restorative dentistry as explained above. Amorphous phase separation of ionomer glasses and fluoro-phospho-silicate glasses, such as the borosilicate glass system, was first studied by Barry et al.

He has acknowledged the division of the separation in two phases, one of which is more susceptible to acid attack [12, 27].

1.3 Structural Characterization of Ionomer glasses by Solid state MAS-NMR Spectroscopy

The structure of complex amorphous and crystalline solid materials is a field of great importance in biomaterials science. These structures are mainly investigated using the technique of solid state MAS-NMR (Magic Angle Spinning Nuclear Magnetic Resonance) [6]. The above glass compositions have been extensively characterised in the past by multinuclear solid state MAS-NMR spectroscopy. It has been suggested that all Si is four fold coordinated and is present as Q^3(3Al) and Q^4(4Al) species. MAS-NMR characterisation of a range of model fluoro-alumino-silicate glasses forming the basis of glass (ionomer) polyalkenoate cements and commercial glasses was focused on four isotopes ^{29}Si, ^{27}Al, ^{31}P and ^{19}F:

^{29}Si: Its spectrum indicates the two following species. Firstly, the Q^3(3Al) species which represent a silicon with one non-bridging oxygen and three Si-O-Al linkages and secondly, the Q^4(4Al) species which represent a silicon with four Si-O-Al bonds.

^{27}Al: It was found predominantly in four-fold coordination except in glasses with high fluorine contents that have also a small proportion of five and six coordinated aluminium.

^{31}P: Its presence is observed as Al-O-PO$_3$, which has a local negative charge of -2. The negative charge is compensated by cations such as Ca^{2+} or six-fold coordinated Al.

[19]F: F-Ca (n) and Al-F-Ca (n) species are found to be present in the calcium based glass compositions. F-M (n) corresponds to fluorine surrounded by n next nearest neighbour cations whereas Al-F-M (n) represents a fluorine bonded to aluminium with the metal M in close proximity, charge balancing the tetrahedral AlO_3F species. An increase in the fluorine content of the glass and lower non-bridging oxygen contents give rise to an increase in the proportion of Al-F-M (n) species [34].

A lot of information has been reported regarding the fluorine environment within the aluminosilicate glass network by the MAS-NMR studies of Stamboulis and Hill [2, 21, 35, 36]. Stamboulis et al. did not justify the presence of Si-F-Ca (n) although its presence cannot be completely ruled out. This is considered as true due to the increasingly stronger peak with fluorine content at -125 ppm observed by high fluorine containing glasses with the general composition of $4.5SiO_2$-$3Al_2O_3$-$1.5P_2O_5$-$(5-x)CaO$-$xCaF_2$ where x = 0-3. Identification of F-Ca(n) and Al-F–Ca(n) species in all glasses at -90 ppm and -150 ppm respectively can also be made.

High concentration of five- and six-fold coordinated Al was observed in the MAS-NMR studies conducted by Stebbins et al [37]. Stabilisation of the high-coordinated Al species by the F[-] ions present in the Al coordination was observed. A series of fluorine containing alumino-silicate glasses and commercial ionomer glasses was additionally tested by applying ^{27}Al and ^{19}F MAS-NMR spectroscopy by Stamboulis et al. and Hill et al. [35, 36]. A lower resonance shift position of the peak of four-fold coordinated Al (IV) for the phosphorus containing glass due to the Al-O-P bonds being formed in contrast to a phosphorus free calcium alumino-silicate glass was found.

1.4 Crystallisation of Ionomer glasses

The last 20 years have been a time of revolution for glass ceramic development [15]. The work of Hill et al led to the development of the SiO_2-Al_2O_3-P_2O_5-CaO-CaF_2 system that crystallises to an apatite phase that is the basis of glass-ceramic bone substitutes and is mainly used in orthopaedic and dental applications. The presence of fluorine in the above system has a significant effect on the nucleation and crystallisation behaviour of the glasses. The system undergoes bulk crystallisation of Fluorapatite (Ca-FAP) and Mullite that followed prior amorphous phase separation. Evidence for the above are the optimum nucleation temperatures and the two loss peaks occurring in dynamic mechanical thermal analysis experiments on nucleated (phase separated) glasses. Often these glasses exhibit two transition temperatures that are identified by the loss peaks in a dynamic mechanical thermal analysis study. When the glasses are phase separated, the first phase is calcium, phosphate and fluoride rich, crystallizing to fluorapatite (first crystallisation temperature) and the second phase is aluminium and silicon rich, crystallizing to mullite (second crystallisation temperature) [27].

APS (amorphous phase separation) is particularly important in glass–ceramics, as it often occurs before crystal nucleation. It is the dominant nucleation mechanism in commercial glass–ceramics and often occurs much faster than a nucleation mechanism involving the precipitation of crystals of a nucleating phase. APS often promotes crystal nucleation by two distinct mechanisms. It can provide an internal surface for heterogeneous crystal nucleation, which will always have lower activation energy than homogeneous nucleation, and it can also result in lowering the activation energy for homogeneous crystal nucleation, as a result of one of the two new

amorphous phases being closer in chemical composition to the crystal phase that forms. Nano-scale APS will often promote crystal nucleation, but may then serve to hinder crystal growth and coarsening, as it will be difficult for a crystal to grow into the second amorphous phase that is depleted in the species forming the crystal phase. This is illustrated schematically in Figure 1.3. In this case there is a strong correlation between the size of the extracted crystals and the size of the droplet phase, suggesting that the Ca-FAP crystals do not grow beyond the boundaries of the droplet phase [39].
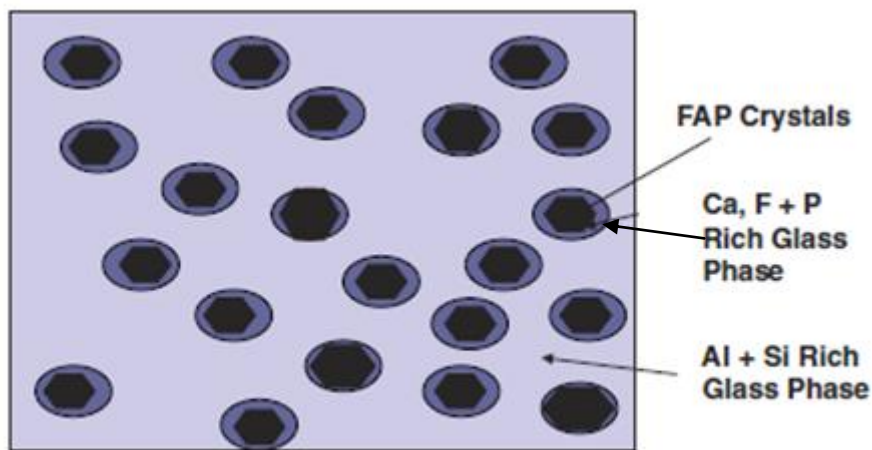
Figure 1.3: The figure indicates the Ca-FAP crystal growth which is inhibited by the size of the droplet. The droplet phase size is equivalent to the fluorapatite crystal size. Reaching the transition temperature of the second phase stimulates the fluorapatite crystal to exceed the droplet phase boundaries [39].

One of the compositions, studied by Dimitrova-Lukacs et al. [16], shows an increase in the material's fracture toughness and strength. The high fracture toughness results from the microstructure, which consists of interlocking apatite and mullite crystals. The apatite crystals can have an aspect ratio >50, and during fracture these needle-like

crystals are pulled out resulting in a high fracture toughness. A microstructure made out of elongated hexagonal apatite crystals is shown in Figure 1.4.
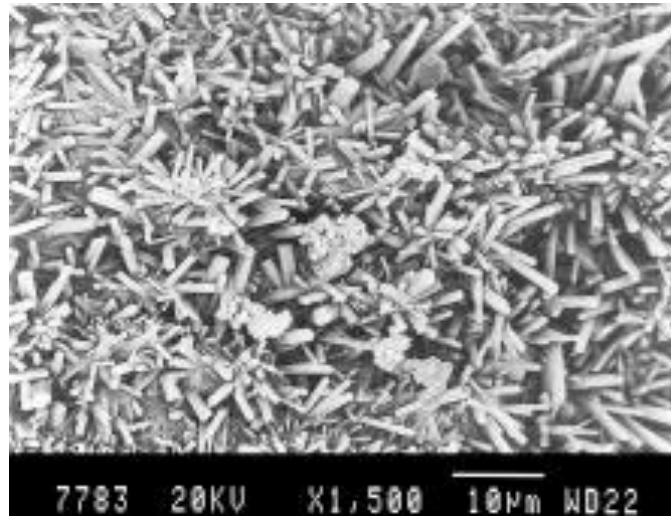
Figure 1.4: SEM of a fracture surface showing elongated apatite crystals with a high length to diameter aspect ratio [16].

Glass-ceramics are divided in three main groups:

1. The Apatite-Wollastonite ceramics [15]

2. Mica-based materials [15]

3. The Apatite-Mullite glass-ceramics[40].

Apatite-wollastonite and Apatite-Mullite systems have apatite as their primary phase and in the case of fluorine containing Apatite-Mullite glass-ceramics the apatite is a Ca-FAP phase. Ca-FAP is more effective as a primary phase in Apatite-Mullite systems for the following reasons:

The fluoride ions in Ca-FAP are smaller than the hydroxyl ions in Hydroxyapatite (HA) hence packing more readily in the lattice. The release of fluoride ions gives out

a cariostatic effect making the system more suitable for tooth saving preparation methods.

Due to the importance of the above, scientists researched on the crystallisation of Apatite-Mullite glass-ceramics. These ceramics have a general composition of $4.5SiO_2-3Al_2O_3-1.5P_2O_5-(5-x)CaO-xCaF_2$ (where x = 0-3.0) with two fluorine atoms substituting for one oxygen atom, which is the basis of the series of ceramics being formed today. A Ca:P ratio of 1.67 representing that in apatite is observed in every glass of this composition. Glasses with x = 0.5 on the other hand, have a Ca:P:F ratio of 5:3:1 representing the stoichiometry in fluorapatite. The substitution of oxygen by fluorine gives a crosslink density of 1.04 for the highest fluorine content possible, 0.44 less than the glass without fluorine as calculated by Ray et al. Fluorine has two roles in glasses, one being that of a nucleating agent leading to the crystallisation of fluorapatite. The other role is the allowance of a motion and rearrangement of the glass network by facilitating the kinetics of crystallisation [16].

1.5 Cation Substitution in Ionomer glasses

Polyalkenoate cements (used for medical and dental applications) are formed by calcium fluoro-alumino-silicate glasses or fluoro-alumino-silicate glasses containing phosphate and strontium. A MAS-NMR study showed that the presence of F-Ca(n) species in the glass is critical for the formation of Ca-FAP [21]. This becomes particularly critical when cation substitution takes place. For example, Mg, Sr and Ba substitution resulted in the presence of F-Mg(3), Al-F-Mg, F-Sr(3), Al-F-Sr and Al-F-Ba species with obvious lack of F-Ba(3). As a result only Mg and Sr substituted glasses crystallised to Wagnerite and Sr-Fluorapatite whereas Ba substituted glasses

did not crystallise to any apatite phase [21, 33, 36]. The latter information gave a better insight in the understanding of the crystallisation mechanism and potential applications of the above systems.

Radio-opacity that makes glasses opaque to X-Rays is introduced to the glass ionomer cements usually by strontium, a substitute for calcium. For instance, the substitution of strontium for calcium was investigated during nucleation and crystallisation of a composition that has a Ca:P ratio of 1.67 corresponding to apatite stoichiometry and crystallizes to Ca-FAP. This was first noticed and studied by Hill and Stamboulis. Strontium can be a substitute to calcium since they have similar ionic radii, 1.16 nm for strontium and 0.94 nm for calcium. Substitution of strontium in crystalline structures may also occur. An example is the substitution of strontium in Apatite structures [2, 12]. Solid solutions of strontium-calcium Hydroxyapatite $(Sr,Ca)_{10}(PO_4)_6(OH)_2$, and pure Strontium Apatite are produced by aqueous solutions and are hence described as minerals. An increase in the unit cell dimensions, with a and c increasing to 0.942 from 0.688 nm for HA occurs when strontium is introduced into the apatite lattice due to the slightly larger ionic radius of strontium. An X-ray diffraction pattern for strontium apatite was produced due to this change with larger d-spacing than its calcium counterpart. A material with increased X-ray radio opacity is produced due to the increased atomic weight and number of strontium which in turn leads to an increased density of both the glass and crystal structure. The ability to observe a materials location and behaviour is basically what is important for medical and dental applications.

Other substitutions studied include Mg and Ba cations. The size of the cations is considered to strongly affect the structure and crystallisation of the ionomer glasses. In Ba-substituted glasses for example, the silicon and phosphorus environment of the glass was not highly influenced by the substitution. Yet, FTIR studies showed that Ba-substitutions have the following effects [11, 42]: 1) A lower inter-tetrahedral angle in Si-O-Si is being formed, 2) A less strained glass network is achieved, 3) Low barium contents affect the crystallisation of the main phases which are Ca-FAP, Mullite and some mixed Ba-Ca-FAP, 4) At high barium contents, there is no Ca-FAP forming during crystallisation but mostly a barium aluminosilicate phase together with crystalline $BaPO_4$.

1.6 Aims and Objectives

The purpose of this research is to study the influence of magnesium substitution on the structure of fluorine containing calcium-alumino-silicate glasses and the resulting glass-ceramics. Consequently, the main purpose of this project is:

- To study how Mg substitution can affect the glass transition temperature (Tg), the crystallisation temperatures (Tp1, Tp2) as well as the optimum nucleation temperature (Tn).

- To understand the crystallisation mechanism and determine the crystal phases as well as the crystal size of each crystal phase.

- To calculate the Activation Energy (Ea) of Ca-FAP/Wagnerite, giving information about the related nucleation and growth process that corresponds to the formation of Ca-FAP.

CHAPTER 2

MATERIALS AND METHODS

2.1 Materials

The study was based on the use of Ca-alumino Silicate glasses with a composition of $4.5SiO_2$-$3Al_2O_3$-$1.5P_2O_5$-$3CaO$-$2CaF_2$ and an excess of fluorine content Ca:P:F = 5:3:1. The production of the alumino-silicate glass of the defined composition occurred using a melt quench route [70]. The required reagents are silica (SiO_2), alumina (Al_2O_3), phosphorus pentoxide (P_2O_5), calcium carbonate ($CaCO_3$) and calcium fluoride (CaF_2). Concerning the Mg – substituted alumino silicate glasses, the composition is $4.5SiO_2$-$3Al_2O_3$-$1.5P_2O_5$-$3CaO$-$2CaF_2$, by LG26(25%)Mg, LG26 (50%)Mg, LG26(75%)Mg and LG26(100%)Mg. The required reagents are silica (SiO_2), alumina (Al_2O_3), phosphorus pentoxide (P_2O_5), calcium carbonate ($CaCO_3$), calcium fluoride (CaF_2), magnesium oxide (MgO) and magnesium fluoride (MgF_2) (all the reagents were of analytical grade and supplied by Sigma-Aldrich)

The following steps were applied for the formation of alumino silicate glass and Mg-substituted alumino silicate glasses:

- A total amount of 500 g of glass was measured and mixed.

- Transfer of the glass batch in a platinum crucible and heating at a temperature of 1475°C for 2 hours.

- The glass melt was then quenched in deionized water to avoid phase separation and crystallization resulting in the formation of frit glass (fritting). The frit glass was then grounded using a pestle and mortar and sieved.

Table 2.1.2: Composition of Mg substituted alumino-silicate glasses

Glass code	Oxides-Molar Composition						
	SiO_2	Al_2O_3	P_2O_5	CaO	CaF_2	MgO	MgF_2
LG26(25%)Mg	4.5	3	1.5	1.75	2	1.25	0
LG26(50%)Mg	4.5	3	1.5	0.5	2	2.5	0
LG26(75%)Mg	4.5	3	1.5	0	1.25	3	0.75
LG26(100%)Mg	4.5	3	1.5	0	0	3	2

2.2 Methods

2.2.1 Helium Pycnometer – Density Measurements

The density of glasses and glass ceramics was measured using the method of helium pycnometer. Gas pycnometry is a common analytical technique that uses a gas displacement method to measure volume accurately. Inert gas, such as helium is used as the displacement medium. The sample is sealed in the instrument compartment of known volume, the appropriate inert gas is admitted, and then expanded into another precision internal volume. The pressure is measured before and after expansion and is

used to calculate the sample volume. Dividing this volume into the sample weight gives the gas displacement density.

The AccuPyc II 1340 Series Pycnometer, that we used for density measurements of glasses and glass ceramics, is automatic and provides density calculations on a wide variety of powders, solids, and slurries having volumes from 0.01 to 350 cm^3. In our case the samples were <45μm of particle size and their mass was approximately 1gr. The instrument completed sample analyses in thirty minutes providing us with 10 consecutive measurements as well as the deviation of each measurement. In order to calculate the density of the glasses and glass ceramics we took the average of these ten consecutive measurements.

In addition, the oxygen density was calculated in order to provide us with an indication of the change of network connectivity with substitution.

Then the oxygen density of glasses was calculated by using the following equation 2.2:

$$Oxygen\ Density = \ Density \ \times \frac{molecular\ weight\ of\ oxygen}{molecular\ weight\ of\ glass} \qquad \text{(Eq 2.2)}$$

2.2.2 Fourier Transform Infrared Spectroscopy

The FT-IR Spectroscopy is used in order to understand the nature of the bonds formed in the amorphous glass with Mg substitution. Fourier transform infrared (FTIR) powder absorption spectra were recorded in the 4000 - 400 cm^{-1} region by using a

Perkin-Elmer FTIR spectrometer (Spectrum 2000, Perkin Elmer, USA). A mixture of the sample and KBr powders in an agate mortar and pestle which was then pressed into the required shape resulted in the production of the KBr pellets. The weight ratio of sample/KBr was 0.01. Approximately 12 scans were shown by the spectrum of each sample represented an average of 12 scans and the background spectrum of a blank KBr pellet was subtracted.

2.2.3 X-ray Powder Diffraction

X-ray Powder Diffraction is used in order to measure the crystal size of the formed Ca-FAP as well as how the crystal size is affected by magnesium substitution. Also, this technique will show the different crystal phases formed with magnesium substitution. An increase in temperature of 10°C per minute up to 1100°C using a ramp heated all the frit glass samples. Once that temperature was achieved the samples were left to heat for an hour and then cooled to room temperature using a furnace. X-Ray diffraction was then performed on the samples using a continuous scan between $2\theta = 10°$ and $60°$, with a step size of $2\theta = 0.0200°$. A Philips analytical x'pert XRD was used with Cu Ka, at 40 kV and 40 mA.

Use of the Scherrer equation calculated the crystal size D [48, 49, 75]:

$$D=K\lambda/[w\cos(\theta)] \qquad\qquad (Eq\ 2.3)$$

K is a constant that takes values between 0.9 and 1.0 depending on the particle morphology. λ is the Cu Kα radiation (0.15406nm), w is the full width at half-maximum (FWHM in radian), and θ is the diffraction angle (in degrees). In this

experiment the average value of K = 0.95 was used giving an average volume of the apparent size independent of the morphology.

2.2.4 Differential Scanning Calorimetry

In order to investigate the nucleation and crystallisation behaviour of glasses or in other words in order to measure the optimum nucleation temperatures a NETZSCH 404C DSC with pairs of matched platinum-rhodium crucibles was used. 20 mg Al_2O_3 were weighed for the reference crucible as well as 20 mg samples were weighed and placed in dry argon followed by heating with a rate of 10^oC/min (unless otherwise stated).

The method outlined by Marotta et al. was followed for the determination of the optimum nucleation temperature in glasses that undergo bulk crystal nucleation [50]:

DSC (Differential Scanning Calorimetry) was used in order to determine the glass transition and crystallisation temperature of glasses. The temperature range was from 25 to 1100^oC and the heating rate was 10^oC/min. The sample weight was ca 20 mg for all samples and the reference sample was alumina. According to the Marotta method [43, 51], the glass sample should be held for 1 hour at 4 different temperatures T_g+20, T_g+40, T_g+60 and T_g+80, and then it should be heated at 10^oC/min to 1100^oC. All the measurements were run at the temperature range of 400°C-1100°C with a heating rate of 10°C/min in a dry argon gas atmosphere. The optimum nucleation temperature was then calculated as the temperature that corresponds to the minimum of the curve

defined by plotting the new first crystallisation temperatures against the holding temperatures.

The number of stable nuclei N_n produced in a sample per time element t_n as indicated by Marotta et al. is:

$$N_n = I \ t_n^b \qquad\qquad \text{(Eq 2.4)}$$

where I is the kinetic rate constant of nucleation and b is a parameter related to the nucleation mechanism. The exothermal crystallisation peak temperatures will reflect variations in nucleation rates when the samples have been subjected to lengthening heating in the surrounding area of the assumed nucleation maxima. The above observation led to Marotta realising that if t_n is the same for each sample at each temperature T_n, the subsequent equation can be applied [52-55]:

$$\ln I = \frac{E_c}{R}\left[\frac{1}{T_p'} - \frac{1}{T_p}\right] + C \qquad\qquad \text{(Eq 2.5)}$$

where E_c is the activation energy for crystallisation, R is the gas constant, T_p' is the crystallisation peak temperature occurring after a nucleation hold, T_p is the latter crystallisation peak temperature without a nucleation hold and C is the constant.

The experiments for the calculations of the activation energy for the crystallisation of fluorapatite were conducted in the Physics Department at Warwick University using the equipment of Mettler Toledo TGA/DSC 1 and Pt crucibles. These calculations using both the Marotta method and the modified Kissinger method as proposed by Matusita *et al.* [40] provide information about the related nucleation and growth process. The Marotta method is based on the equation 2.6:

$$Ln\ {}^1\!/_r = E_C / RT_P + C \qquad\qquad \text{(Eq 2.6)}$$

where r is the heating rate, E_C is the activation energy of the process, T_P is the temperature corresponding to the maximum of the crystallisation peak, R is the universal gas constant, and C is the constant.

On the other hand, the modified Kissinger method suggested by Matusita and Sakka [54] is based on the equation 2.7:

$$Ln\left(T_P^2 / r^n\right) = mE_C / RT_P + C \qquad\qquad \text{(Eq 2.7)}$$

where T_P is the crystallisation peak temperature, r is the heating rate, R is the universal gas constant, n and m are the numerical constants which depend on the crystallisation mechanism, and C is the constant. For surface nucleation n = m = 1 whereas for bulk nucleation from a constant number of nuclei n = m = 3 and for bulk nucleation from an increasing number of nuclei n=4 and m=3.

The glass composition undergoes no change during crystallisation as assumed by both methods. This is not true when the glass compositions differ to the crystalline phases formed during crystallisation. The Kissinger [55] method makes it possible to assume which are the appropriate values for n and m used for the above calculations including the rare use of non-integer values (such values are used when neither pure bulk nucleation nor surface nucleation occurs). Heating coarse glass particles in five different heating rates which include 2, 5, 10, 15, and 20°C/min was used to calculate the activation energies obtained.

CHAPTER 3

RESULTS

3.1 Effect of Cation Substitution on Glasses.

3.1.1 Density and Oxygen Density of Mg Substituted Glasses

The measured density and oxygen density for Mg containing alumino-silicate glasses are shown in Figure 3.1 and Figure 3.2. It is indicated, that the decrease of density is proportional to the enhancement of magnesium substitution with the highest density for LG26 ($4.5SiO_2$-$3Al_2O_3$-$1.5P_2O_5$$3CaO$-$2CaF_2$) at 2.73 g/cm^3 and the lowest density for LG26(100%)Mg ($4.5SiO_2$-$3Al_2O_3$-$1.5P_2O_5$-$3MgO$-$0.75MgF_2$-$1.25CaF_2$) at 2.65 g/cm^3.
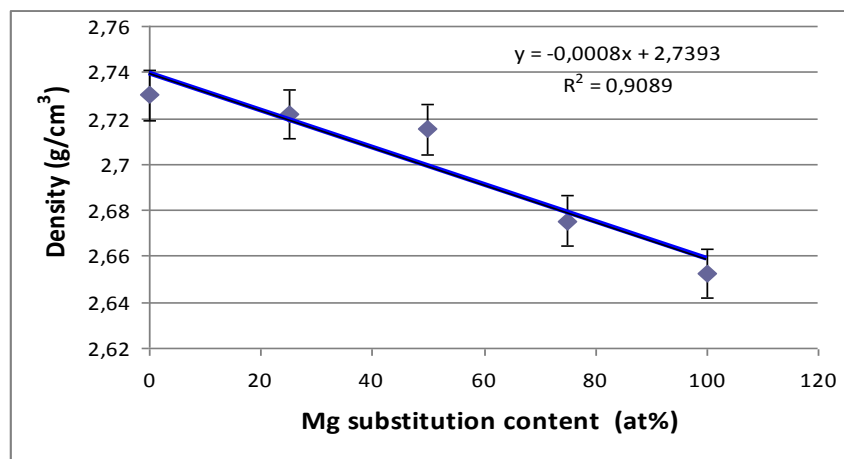

**Figure 3.1:** Density of Mg containing glasses.
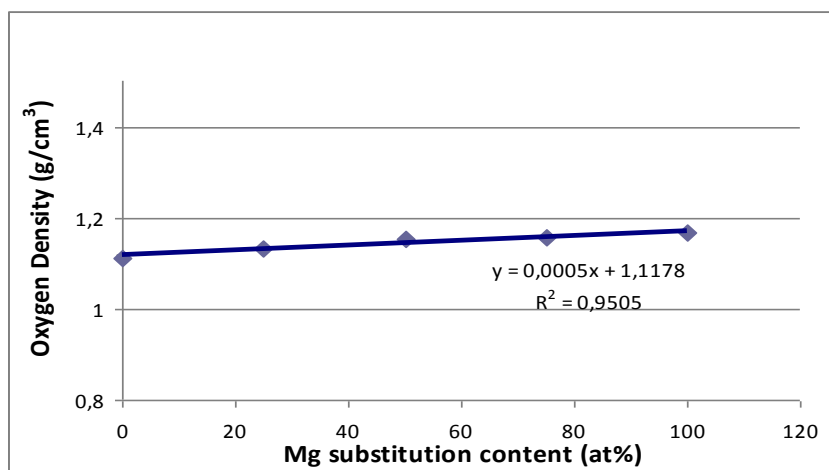
Figure 3.2: Oxygen Density of Mg containing glasses.

However, the oxygen density, based on the density values mentioned above, shows a slightly increasing tendency, suggesting that there is a very small change of the oxygen environment within the glass network with Mg substitution. The oxygen density is increased from 1.11 g/cm^3 for LG26 to 1.17 g/cm^3 for LG26(100%)Mg.

3.1.2 FTIR analysis of Mg substituted glasses

Figure 3.3 shows the FTIR adsorption spectra of all Mg containing glasses. The first strong bands in the region of 800-1400 cm^{-1} appear in all samples and are assigned to the Si-O(s) and P-O(s) stretching vibrations, however with increasing the Mg molar content from LG26 to LG26(100%)Mg, these bands are shifted to slightly higher wavenumbers, i.e., from 1089 cm^{-1} to 1109 cm^{-1} [56, 57]. In the case of LG26(100%)Mg there is a difference, the bands are shifted to slightly lower wanenumbers. It is very likely that this happens due to the more tight glass network formed with 100%Mg substitution. In addition, there is an effect in the intensity of the band situated at around 983 cm^{-1} that decreased with increasing the Mg molar content

in the glass. Furthermore, there is a medium strong band in the region of 620-800 cm^{-1} which is associated with AlO_4 tetrahedra. The band between 530-620 cm^{-1} is attributed to the P-O bending vibrations and Si-O-Al linkages, while the band centred at around 460 cm^{-1} is related to the motion of bridging oxygens in the plane perpendicular to the Si-O-Si(Al) bond, in other words is attributed to vibrations of the Si-O-Si and Si-O-Al bonds [58- 60].
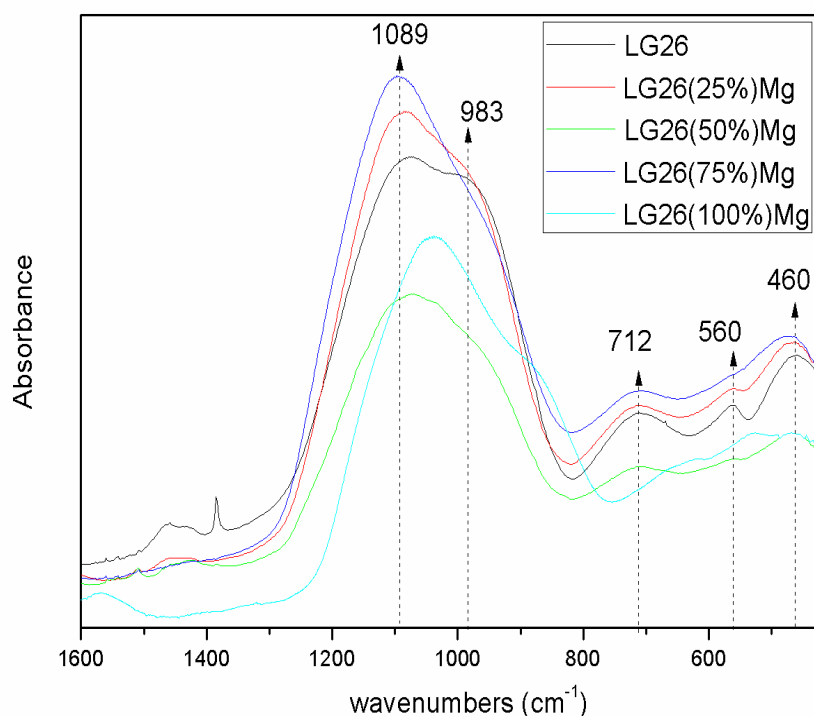

Figure 3.3: FTIR spectra of all Mg substituted glasses.

3.1.3 Glass Transition and Crystallization Temperatures of Mg Substituted Glasses

Coarse particles (>45μm) of Mg containing glasses were characterised by using differential scanning calorimetry (DSC) at a heating rate of 10°C/min from room temperature to 1100°C. All graphs showing glass transition temperatures and

crystallisation peak temperatures are presented in Figure 3.4 and Figure 3.5. Table 3.1 presents the values of glass transition and crystallisation temperatures for all glasses. It is clear that in these glasses, the corresponded glass transition temperature (Tg) of LG26 has the highest value of 655°C whereas the Tg of each sample (LG26(25%)Mg, LG26(50%)Mg, LG26(75%)Mg, LG26(100%)Mg) is decreased initially with increasing the content of Mg, but then increased when the content of Mg is higher than that of Ca.
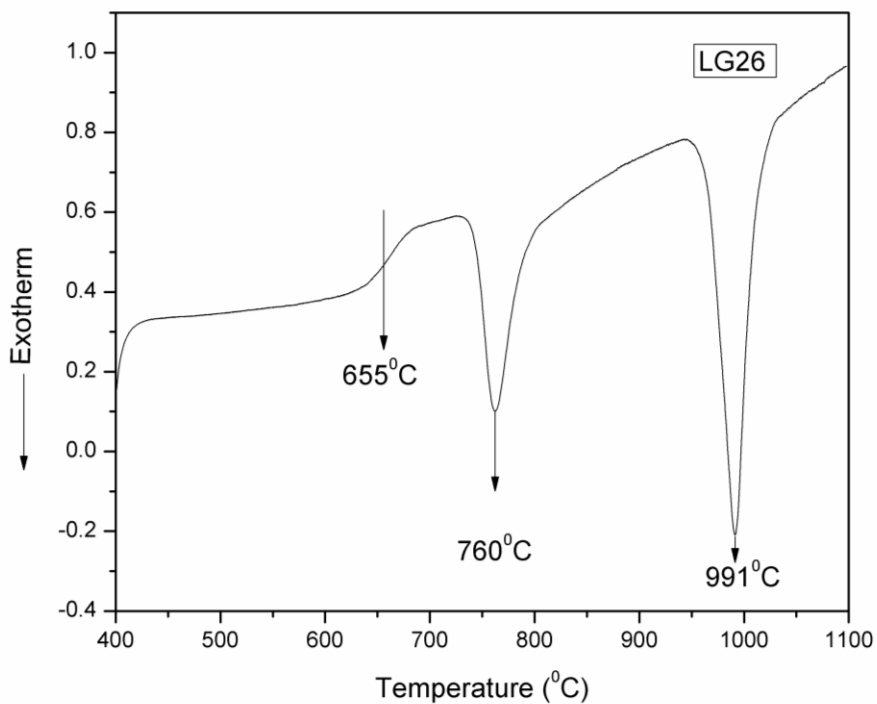
**Figure 3.4:** DSC trace of calcium containing glass LG26 with particle size >45μm measured at a heating rate of 10°C/min.

Concerning the first crystallisation peak temperature (Tp1) the progressive Mg substitution forces Tp1 consistently to higher values from 760°C in the case of LG26 to 983°C in the case of LG26(100%)Mg as shown in Table 3.1. It is suggested, that

the changes of Tp1 in Mg substituted glasses may be related to the formation of different crystalline phases at Tp1 in each sample.
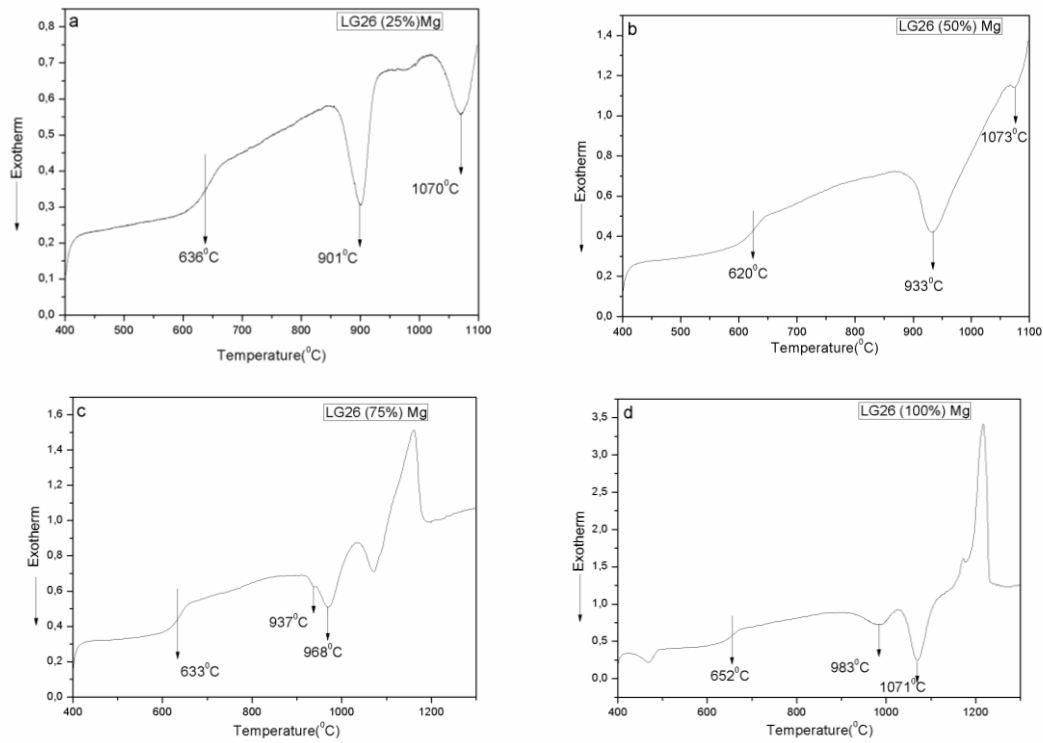
Figure 3.5: DSC traces of all Mg containing glasses (a) (LG26(25%)Mg, (b) LG26(50%)Mg, (c) LG26(75%)Mg and (d) LG26(100%)Mg) with particle size ranging from 3mm to 45μm-100 μm measured at a heating rate of 10°C/min.

Table 3.1: DSC analysis data for all Mg containing glasses (particle size >45μm) measured at a heating rate of 10°C/min.

Glass	Mg content (at%)	Tg(^{o}C)	Tp1(^{o}C)	Tp2(^{o}C)
LG26	0	655	760	991
LG26(25%)Mg	25	636	901	1070
LG26(50%)Mg	50	620	933	1073
LG26(75%)Mg	75	633	937	968

LG26(100%)Mg	100	652	983	1071

The second crystallisation peak temperature (Tp2) on the other hand increases initially from 991°C in the case of LG26 to 1070°C in the case of LG26(25%)Mg and 1073°C in the case of LG26(50%)Mg but then decreases to 968°C in the case of LG26(75%)Mg but increases again to 1071°C in the case of LG26(100%)Mg. A characteristic endotherm at around 1200°C is observed in graphs 3.5c and d most likely associated with crystal dissolution.

3.2 Effect of Cation Substitution on Glass-Ceramics

3.2.1 Density of Mg Substituted Glass-Ceramics

Figure 3.6 shows the measured density of Mg substituted glass ceramics. It is clear, that the density for glass ceramics is decreased slightly with Mg substitution from 2.88 g/cm^3 for LG26 (4.5SiO$_2$-3Al$_2$O$_3$-1.5P$_2$O$_5$3CaO-2CaF$_2$) to 2.84 g/cm^3 for LG26(100%)Mg (4.5SiO$_2$-3Al$_2$O$_3$-1.5P$_2$O$_5$-3MgO-0.75MgF$_2$-1.25CaF$_2$).
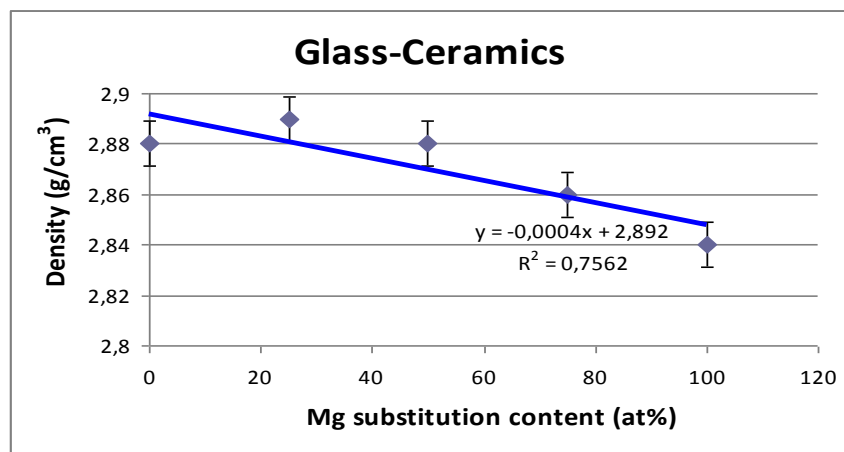
Figure 3.6: Density of Mg containing glass ceramics.

It is observed, there is a linear relationship between the density and Mg molar content. In addition, in this case the density depends on the amount and type of phases formed in glass-ceramics.

3.2.2 XRD Study of Mg substituted Glass-Ceramics

Figure 3.7 indicates the X-Ray powder diffraction analysis of Mg substituted glasses heat treated up to $1100^{o}C$ with one hour hold in optimum nucleation temperature. It is observed that the formation of Wagnerite (Mg_2PO_4F) (JCPDS 00-042-1330) is favoured with increasing Mg substitution and fully replaces Ca-FAP when the Mg content is higher than that of Ca.
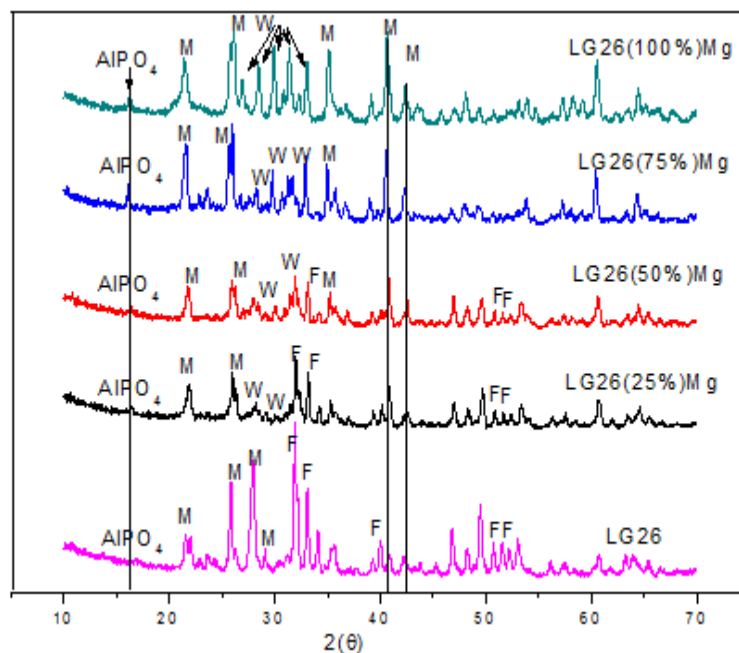
Figure 3.7: X-ray powder diffraction patterns of heat treated Mg glass-ceramics. F = Ca-FAP, M = Mullite, W = Wagnerite.

In particular, Mullite ($Al_6Si_2O_{13}$) is present in all crystallised samples, Ca-FAP ($Ca_5(PO_4)_3F$) appears in LG26 in LG26(25%)Mg and in LG26(50%)Mg while Wagnerite (Mg_2PO_4F) is present in all substituted glass-ceramics apart form LG26 as shown in Table 3.2. There is also a small amount of $AlPO_4$ present. The LG26 containing glass is mainly crystallised to Ca-FAP and Mullite as well as a small amount of $AlPO_4$.

Table 3.2: Analysis of XRD patterns of different Mg containing glass-ceramics.

GLASS	CRYSTAL PHASES			
LG26	$Ca_5(PO_4)_3F$	x	$Al_6Si_2O_{13}$	$AlPO_4$
LG26(25%)Mg	$Ca_5(PO_4)_3F$	Mg_2PO_4F	$Al_6Si_2O_{13}$	$AlPO_4$
LG26(50%)Mg	$Ca_5(PO_4)_3F$	Mg_2PO_4F	$Al_6Si_2O_{13}$	$AlPO_4$
LG26(75%)Mg	x	Mg_2PO_4F	$Al_6Si_2O_{13}$	$AlPO_4$
LG26(100%)Mg	x	Mg_2PO_4F	$Al_6Si_2O_{13}$	$AlPO_4$

Furthermore all Mg substituted glasses were heat treated up to corresponding Tp1 and studied by XRD analysis in order to identify the crystal phases formed at Tp1. The Tp1 used for the heat treatments was measured from the DSC curves shown in Figure 3.11 (a, b, c and d) and used to calculate the activation energy (with holding at the optimum nucleation temperature) when the heating rate was 10^oC/min. Figure 3.8 shows that Ca-FAP ($Ca_5(PO_4)_3F$) and Wagnerite (Mg_2PO_4F) are formed at Tp1 in LG26(25%)Mg containing glasses, while only Wagnerite (Mg_2PO_4F) is formed in LG26(75%)Mg glass-ceramic at Tp1.
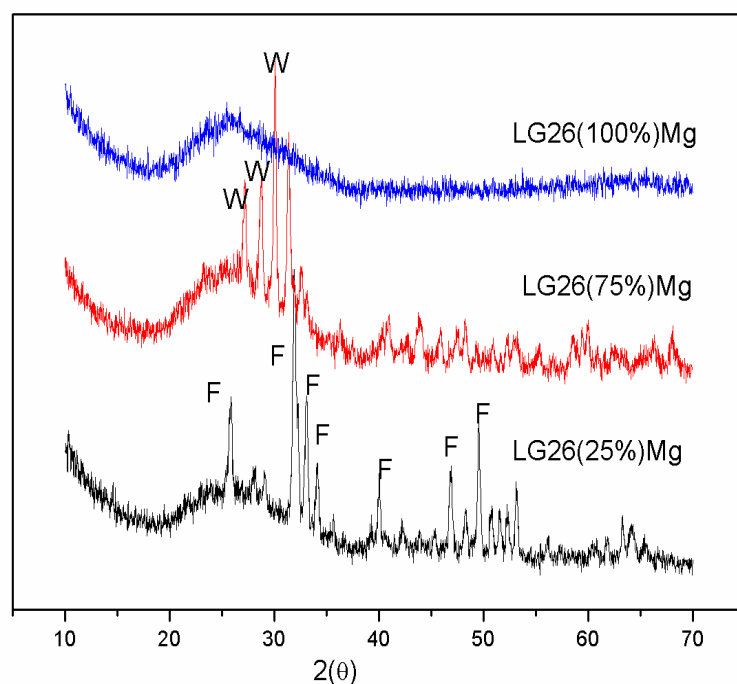
Figure 3.8: X-ray powder diffraction patterns of heat treated Mg glass-ceramics up to Tp1. F = Ca-FAP, W = Wagnerite.

Table 3.3: Comparison of the crystal size and type of Ca-FAP ($Ca_5(PO_4)_3F$), Wagnerite ($Mg_2(PO_4)F$) and Mullite ($Al_6Si_2O_{13}$) phase formed in glass-ceramics with different Mg content.

GLASS	CRYSTAL SIZE (nm)		
	Ca-FAP ($Ca_5(PO_4)_3F$) **Hexagonal**	**Mullite** ($Al_6Si_2O_{13}$) **orthorhombic**	**Wagnerite** ($Mg_2(PO_4)F$) **Monoclinic**
LG26	28	26	x
LG26(25%)Mg	84	53	34
LG26(50%)Mg	26	72	42
LG26(75%)Mg	x	59	35
LG26(100%)Mg	x	31	30

In the case of LG26(100%)Mg the XRD pattern showed that the glass was not crystallised to Wagnerite at the temperature indicated by DSC (Figure 3.11(d) below) as the first crystallisation temperature. It is therefore concluded that the first crystallisation temperature is higher than the above temperature and corresponds to the second exothermic transition observed in Figure 3.11(d). The crystal size of all phases, such as Ca-FAP ($Ca_5(PO_4)_3F$), Wagnerite (Mg_2PO_4F) and Mullite ($Al_6Si_2O_{13}$), was calculated by the Scherrer equation and is shown in Table 3.3.

3.2.3 Optimum Nucleation Temperature and Activation Energy Study on Mg Substituted glasses

As described before in Chapter 2, the Marotta method was used in order to calculate the optimum nucleation temperatures for Mg substituted glasses. As it has been mentioned, the minimum point in the curve of the first crystallisation temperatures Tp'1 against the nucleation temperature Tn, corresponds to the optimum nucleation temperature. For example, Figure 3.9 shows the DSC traces for LG26(25%)Mg after 1 hour hold at different nucleation temperatures e.g. $656^{o}C$, $676^{o}C$, $696^{o}C$ and $716^{o}C$. The Tp'1 for the four different nucleation temperatures is $840^{o}C$, $832^{o}C$, $855^{o}C$ and $864^{o}C$, respectively. According to Figure 3.10 the optimum nucleation temperature (Tn) is $671^{o}C$, $658^{o}C$, $654^{o}C$ for LG26(25%)Mg, LG26(50%)Mg and LG26(75%)Mg, respectively.
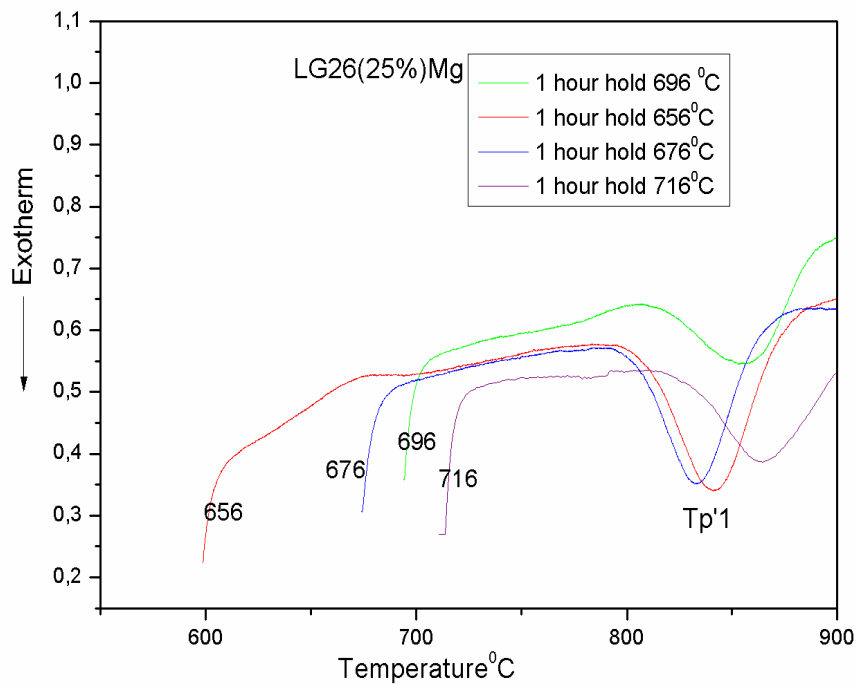
Figure 3.9: DSC traces of LG26(25%)Mg glass with 1 hour hold at different nucleation Temperatures (656˚C, 676˚C, 696˚C, 716˚C) and a heating rate of 10ºC/min.
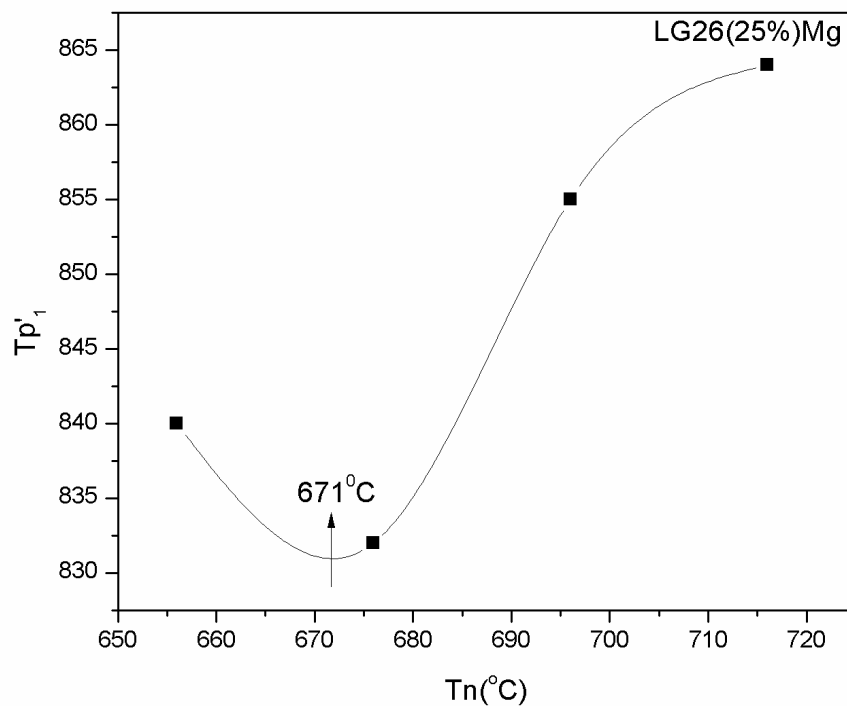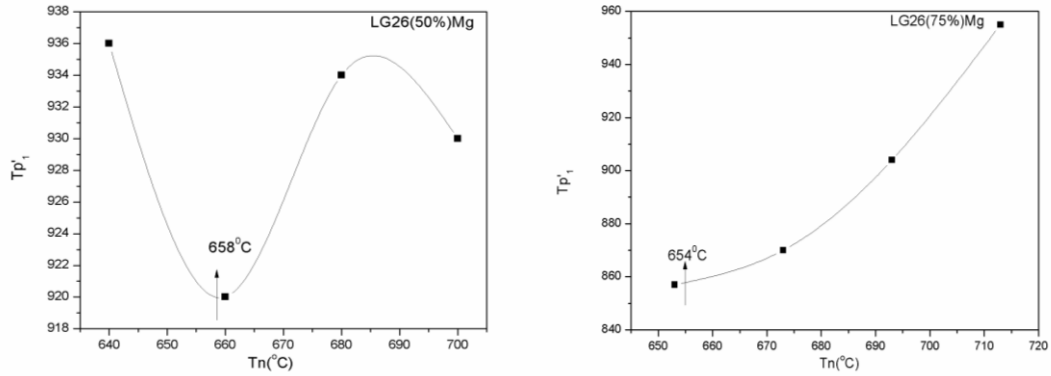
Figure 3.10: Optimum Nucleation curves of Tp´$_1$ collected for the LG26(25%)Mg, LG26(50%)Mg and LG26(75%)Mg containing glasses.

All Mg substituted glasses exhibit well defined optimum nucleation temperatures as Figure 3.10 shows, except for LG26(100%)Mg substituted glass that does not exhibit a well defined nucleation minimum indicating possible phase separation. In particular the LG26(100%)Mg substituted glass crystallises spontaneously, this means that the crystallisation occurs very slowly and it was not possible to calculate the optimum nucleation temperature. When crystallisation occurs slowly then crystallisation is inhibited but the glass is crystallized. All the values of the optimum nucleation temperature (Tn) are indicated in the Table 3.4. It is observed that the optimum nucleation temperatures (Tn) decrease as Mg substitution increases i.e. the value decreases initially from 700°C in the case of LG26 to 671°C in the case of LG26(25%)Mg but then decreases again to 658°C in the case of LG26(50%)Mg and finally results in 654°C in the case of LG26(75%)Mg.

The activation energy (Ea) of Ca-FAP/Wagnerite was determined by the Marotta and Kissinger methods, with or without 1 hour hold in optimum nucleation temperature, respectively. In particular, the activation energy (Ea) of Ca-FAP for LG26(25%)Mg,

LG26(50%)Mg and the Ea of Ca-FAP/Wagnerite for LG26(75%)Mg was determined following 1 hour hold in 671°C, 658°C, 654°C , respectively, using five different heating rates such as 2, 5, 10, 15 and 20°C/min as is indicated in Figure 3.11.
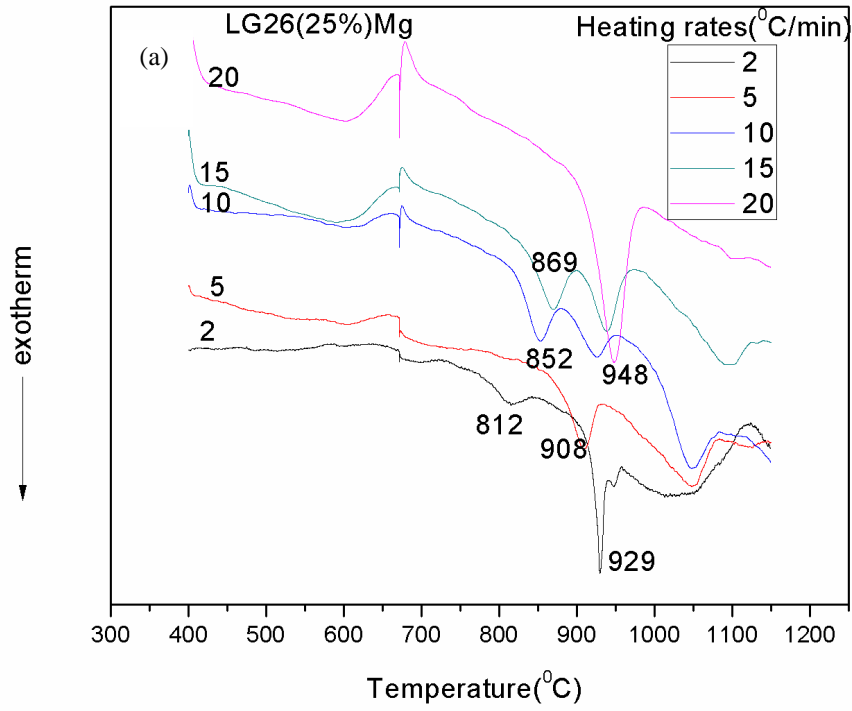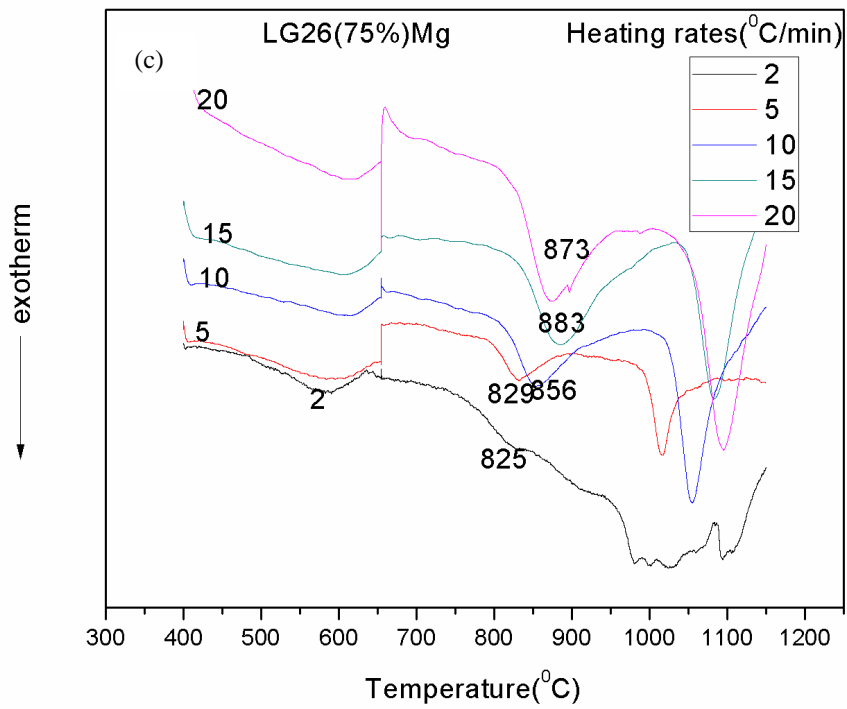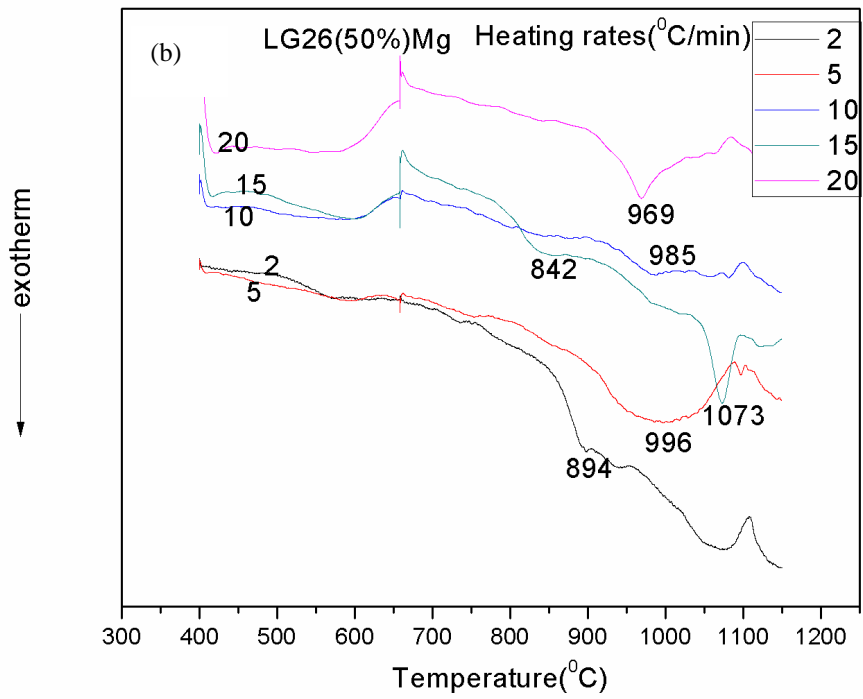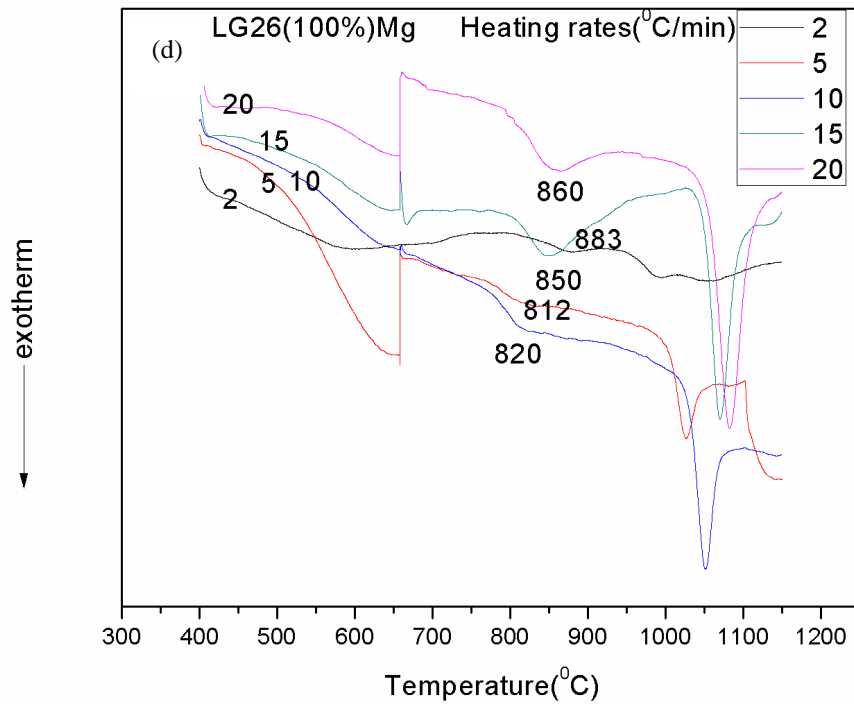
Figure 3.11: DSC traces of (a) LG26(25%)Mg, (b) LG26(50%)Mg, (c) LG26(75%)Mg and (d) LG26(100%)Mg glasses at five different heating rates after 1 hour of optimum nucleation hold.

It is obvious that in the case of LG26(100%)Mg the activation energy (Ea) of Ca-FAP/Wagnerite was not calculated since the glass does not exhibit well defined optimum nucleation temperature. Furthermore, it was observed that the activation energy slightly increased with the exception of LG26(75%)Mg. In order to understand how magnesium substitution can affect the activation energy of Ca-FAP/Wagnerite phase, both the Marotta and Kissinger methods were used for calculations for all Mg substituted glasses (Table 3.4).

Table 3.4: Optimum nucleation temperature and activation energies in Mg containing glasses for Ca-FAP/Wagnerite crystallisation determined by the Marotta and Kissinger method (Matusita)

Glass	Mg substitution content (at%)	Optimum Tn (^oC)	Marotta, Ea (KJ/mol)	n m	Kissinger(Matusita), Ea (KJ/mol)
LG26	0	700	533	3 3	527
		No hold	603	4 3	354
LG26(25%)Mg	25	671	620	3 3	663
		No hold	627	4 3	400
LG26(50%)Mg	50	658	645	3 3	690
		No hold	635	4 3	411
LG26(75%)Mg	75	654	621	3 3	655
		No hold	636	4 3	412
LG26(100%)Mg	100	N	N		N

CHAPTER 4

DISCUSSION

4.1 Effect of Cation Substitution on Glasses

4.1.1 Density and Oxygen Density

The measured density values are decreased linearly with increasing the molar content of Mg from 2.73 g/cm^3 of LG26 glass to 2.65 g/cm^3 of LG26(100%)Mg containing glass shown in Figure 3.1. The substitution of Mg for Ca resulted in a decrease of the density of glasses as Mg has a smaller atomic weight (AW=24.3) and ionic radius (0.065nm) compared to the atomic weight (AW=40) and ionic radius (0.114nm) of Ca. Since the atomic weight of Mg and Ca are significantly different, the linear decrease of density indicates that the atomic weight change has a more important effect on the density values than the ionic radius.

 The oxygen density values on the other hand, increased as the Mg substitution increased, as shown in Figure 3.2. The minimum value is 1.113 g/cm^3 in the case of LG26 and the maximum value is 1.168 g/cm^3 in the case of LG26(100%)Mg. In the glass network, the oxygen density reflects the degree of packing of the atoms. There is a slight linear increase in the oxygen density from LG26 to LG26(100%)Mg containing glasses indicating a closer packed glass network. To summarise, it is clear that Mg substitution leads to a decrease in glass density and an increase in oxygen density.

4.1.2 Fourier Transform Infrared Spectroscopy

The Figure 3.3 showed the FTIR spectra of Mg substituted alumino silicate glasses. The lack of sharp peaks in the FTIR spectra shown in Figure 3.3 indicates a disorder in the silicate network reflecting the wide distribution of Q^n units occurring in the glasses. J.Serra et al. [70] reported that the peak at around 800 cm^{-1} is associated with the bending Si-O(b) vibration whereas the asymmetric Si-O(s) stretching mode is located in the range of 100-1300 cm^{-1}. It was also reported that the symmetric and asymmetric stretching modes of Si-O-Si bonds in the Q^n units appear in the 800-1300 cm^{-1} region with the absorption bands of the Q^n units with n= 4, 3, 2, 1 and 0 centred around 1200, 1100, 950, 900 and 850 cm^{-1}, respectively [65]. As reported from the literature [57] in a simple silica glass all the silicon atoms are bonded to four oxygen atoms and all oxygen atoms are bridging oxygen atoms (BO), each oxygen atom bridges two silicon atoms. In addition, in FTIR spectra, the main absorption band is in the range of 800-1400 cm^{-1} and indicates a distribution of Si-O-Si stretching (Q^4), Si-O-Si stretching (Q^3) and Si-O-[NBO] per SiO_4 tetrahedron (Q^3) [64].

In general, Mg acts as network modifier and can induce a visible shift of certain bands, indicating a change in the formation of non-bridging oxygens in the glass network. The replacement of Mg for Ca results in a shift towards larger wavenumbers for the bands as well as in decreased relative intensity connected with Si-O-NBO bonds. By increasing the Mg content, it is suggested that Mg substitution for Ca leads to the formation of more bridging-oxygens within the glass network, as well as bigger inter-tetrahedral angle values [60]. As observed from the Figure 3.3 the spectra of LG26(100%)Mg substituted glass has a different tendency from all the other spectra. The bands of this spectra are shifted to lower wavenumbers. It is most likely that this

happened due to the more tight glass network formed with 100%Mg substitution. Generally, the formation of more Si–O–NBOs and the breakage of Si–O–Si bonds play an important role in the biological response at the interface of the bioactive materials when exposed to body fluids, therefore the study of the bonding configuration is a key step for the development of new glasses and their biomedical application [60-64].

4.1.3 Glass Transition and Crystallization Temperatures of Mg Substituted Glasses

As indicated in Table 3.1 the glass transition temperature (Tg) decreases slightly with Mg substitution in the beginning and then increases due to the "mixed cation effect" as has been reported elsewhere [68]. Generally, it is observed that the glass transition temperature (Tg) does not change significantly with Mg substitution. It has been reported, that Mg substitution resulted in an increase in the number of bridging oxygens and therefore the network connectivity was expected to increase [11, 21]. However, it is not clear whether an increase in the number of bridging oxygens is connected with an increase in the glass transition temperature. One would expect that an increase in the number of non-bridging oxygens would result in a stiffer glass network and therefore in an increase in the glass transition temperature but the present and previous experimental work [44] has not justified the above assumption. Furthermore, it was observed that both Tp1 and Tp2 increased with Mg substitution. In general, there are not significant changes in Tp1 and Tp2 among Mg substituted glasses but there are significant changes between LG26 and Mg substituted glasses. The values increase or decrease slightly by changing the substitution and often this

behaviour has been characterised as mixed cation effect. It has been reported [65] that the mixed cation effect can represent the nonlinear variation of physical properties (e.g. high minimum conductivity) that was observed in a family of glasses when the relative proportion of two modifiers was varied while the total modifier concentration was kept unchanged. This was most likely related to the cation movement and structural properties. Rao et al. [66] reported, that the glass transition temperature of xK$_2$O–(40−x)Na$_2$O–50B$_2$O$_3$–10As$_2$O$_3$ system exhibits a negative deviation from linearity. For glasses containing 40 mole% of alkali content, the Tg followed the order Na>K that is Tg,$_{Na}$ > Tg,$_K$. In addition, a similar observation was made in silicate glasses and mixed crystals [67]. Other published work [68] showed that the glass transition temperature of glasses containing one network modifier increased in the following order: Na$_2$O<BaO<MgO. This is also consistent with an increase in the cation-oxygen bond strength in the above order. In our case however a similar behaviour was not observed. According to the literature, one would expect that the glass transition temperature would increase with Mg substitution and considering that the cation-oxygen bond is stronger than Ca-O, the Mg substituted glasses should show an increase in the glass transition temperature. Previous work with similar Ba substitutions did not show any increase in the glass transition temperature not even compared to the present data [38]. In the contrary, the glass transition temperature is very similar for both Ba and Mg substitutions. Here it is obvious that the mixed cation effect is not that strong although there is some evidence of the mixed cation effect in the first crystallisation temperature (Tp1). Different models [65] have been used to interpret the mixed cation effect, assuming either a large structural modification induced by mixing mobile species of different sizes or a specific interaction between dissimilar mobile species. Pevzner et al. [68] studied the RO(R$_2$O) · 2B$_2$O$_3$ glasses

(where R_2O = Na_2O, RO = BaO, MgO) upon replacement of Na_2O by BaO or MgO, and BaO by MgO and supported that the mixed cation effect was associated with the difference in energy of cation-oxygen bonds and a different effect of cations on the coordination state of boron.

4.2 Effect of Cation Substitution on Glass-Ceramics

4.2.1 Density of Glass Ceramics

The measured density values for glass ceramics are decreased with increasing the molar content of Mg from 2.88 g/cm^3 of LG26 containing glass ceramic to 2.84 g/cm^3 of LG26(100%)Mg containing glass ceramic, shown in Figure 3.6. This happens because the density depends on the kind of phases as well as the amount of each phase that is present in the glass ceramic. For instance, it has been calculated from the XRD data base (icdd) in x'pert high score that the density of crystal phases such as Ca-FAP ($Ca_5(PO_4)_3F$) with reference code (00-015-0876), Wagnerite (Mg_2PO_4F) with reference code (00-042-1330) and Mullite ($Al_6Si_2O_{13}$) with reference code (00-015-0776) are 3.15 g/cm^3, 3.13 g/cm^3 and 3.00 g/cm^3, respectively. Consequently, it can be explained why the LG26(100%)Mg substituted glass ceramic has the lowest density value while the LG26(25%)Mg substituted glass ceramic has the highest value. According to Table 3.2, it was observed that the LG26 glass ceramic consist of 3 crystal phases such as Ca-FAP, Mullite and $AlPO_4$ whereas the LG26(100%)Mg substituted glass ceramic consists of Wagnerite, Mullite and $AlPO_4$. Gradually the density decreases as the Mg substitution increases since Wagnerite replaces Ca-FAP as well as the density of Wagnerite is lower than the density of Ca-FAP.

4.2.2 XRD Study of Mg substituted Glass-Ceramics

As Figure 3.7 showed, in the first series of measurements that Mg substituted glasses heat treated up to 1100°C with one hour hold in optimum nucleation temperature, the LG26 containing glass is mainly crystallised to Ca-FAP and Mullite ($Al_6Si_2O_{13}$) as well as a small amount of $AlPO_4$. Consequently, the first crystallised phase is the Ca-FAP and the second crystallised phase is the Mullite ($Al_6Si_2O_{13}$). In particular, the introduction of Mg for Ca results in the formation of Wagnerite (Mg_2PO_4F), Ca-FAP and Mullite ($Al_6Si_2O_{13}$) in the case of LG26(25%)Mg and LG26(50%)Mg containing glass ceramics whereas the formation of Wagnerite (Mg_2PO_4F) and Mullite ($Al_6Si_2O_{13}$) is appeared in the case of LG26(75%)Mg and LG26(100%)Mg containing glass ceramics. As was mentioned the formation of cubic $AlPO_4$ phase is detected in all Mg containing glass ceramics. $AlPO_4$ has also been confirmed by Neutron Diffraction [39] by previous work in the case of LG26. As far as the formation of Magnesium Fluoride Phosphate ($MgPO_4F$) is concerned this phase was appeared only in the case of the LG26(75%)Mg containing glass ceramics.

By using Scherrer equation [69, 70], in the first series of measurements that involved heat treatment of Mg substituted glasses up to 1100°C with one hour hold in optimum nucleation temperature (Table 3.2), the crystal size of hexagonal Ca-FAP was calculated to be in the range of 84 to 26 nm, and the crystal size of orthorhombic Mullite was calculated in the range of 31 to 72 nm while the crystal size of monoclinic Wagnerite was in the range of 30 to 42 nm.

Furthermore, all Mg substituted glasses were heat treated up to corresponding Tp1 and studied by XRD in order to identify the crystal phases formed at Tp1. As Figure

3.8 shows the Ca-FAP ($Ca_5(PO_4)_3F$) is produced in LG26(25%)Mg containing glass ceramic whereas the Wagnerite (Mg_2PO_4F) is formed in LG26(75%) Mg containing glass ceramics. In the case of LG26(100%)Mg the XRD pattern showed that the glass was not crystallised to Wagnerite at the temperature indicated by DSC (Figure 3.11(d)) as the first crystallisation temperature. It is therefore concluded that the first crystallisation temperature is higher than the above temperature and corresponds to the second exothermic transition observed in Figure 3.11(d). In order for the LG26(100%)Mg to crystallise the heat treatment should have been conducted to higher temperature (983^oC from Figure 3.5(d)) and not at 820^oC taken from the DSC curve used for the calculation of the activation energy.

4.2.3 Optimum Nucleation Temperature and Activation Energy Study on Mg Substituted glasses

The basic method in order to calculate the optimum nucleation temperature is the method outlined by Marotta et al. as mentioned before. The optimum nucleation curves of Tp'_1 collected for the LG26(25%)Mg, LG26(50%)Mg and LG26(75%)Mg glasses are shown in Figure 3.10. The optimum nucleation temperatures (Tn) decreased as Mg substitution increased. Consequently, a well defined optimum nucleation temperature was calculated for all samples according to the first crystallisation peak temperature except for the LG26(100%)Mg containing glass which does not exhibit an optimum nucleation temperature. It is likely that this glass was phase separated and crystallisation occurred spontaneously without going through the nucleation process. In other words the crystallisation occurs very slowly and it was not possible to calculate the optimum nucleation temperature. When

crystallisation occurs slowly then crystallisation is inhibited but the glass is crystallized. In order to establish whether the above glass was phase separated an X-ray diffractogram of the glass was taken which did not show any sign of crystallisation. Knowing that phase separation can happen at a very small scale it is possible that the XRD shows an amorphous glass pattern. A similar behaviour was observed in previous work [38] with LG26(100%)Ba containing glass which did not appear to have a well defined optimum nucleation temperature, indicating possibly the efficiency of the corresponding phase ($BaAl_2Si_2O_8$) to self-nucleate and grow. Concerning the fact that in all cases the optimum nucleation temperature is only slightly above the glass transition temperature, is indicative of the nucleation mechanism involving amorphous phase separation [39]. It is very important to notice that in the case of LG26(25%)Mg and LG26(50%)Mg the first crystallisation temperature corresponds to the crystallisation of both Ca-FAP and Wagnerite whereas in the case of LG26(75%)Mg and LG26(100%)Mg the first crystallisation temperature corresponds to the crystallisation of Wagnerite only. Therefore in the two first glass compositions the activation energy corresponds to both Ca-FAP and Wagnerite crystal phases with Ca-FAP being the dominant crystalline phase.

As described above in Chapter 2, the calculations of the activation energies of Ca-FAP/Wagnerite crystallisation were conducted using both the Marotta method and the modified Kissinger method as proposed by Matusita *et al.* [40] that give information about the related nucleation and growth process that corresponds to the formation of Ca-FAP/Wagnerite. The values of n=3 and m=3 assume bulk nucleation from a constant number of nuclei for samples with a nucleation hold, while the values n=4 and m=3 assume bulk nucleation from an increasing number of nuclei without a

nucleation hold. The activation energy for all Mg substituted glasses increased compared to the activation energy for Ca-FAP crystallisation of the base LG26 glass whereas the activation energy of Ca-FAP/Wagnerite did not change significantly with Mg substitution if compared to all Mg substituted glasses (some slight increase or decrease in value that do not follow a specific pattern). The increase of the activation energy of Ca-FAP/Wagnerite with Mg substitution compared to the activation energy of Ca-FAP/Wagnerite of LG26 is related with the gradual replacement of Ca-FAP by Wagnerite as Mg substitution progressively increased. In a previous study it was reported that the activation energy corresponding to the crystallisation Ca-FAP in Ba and Sr glasses reduced with increasing substitution of Ba or Sr for Ca. Additionally, the Ba substituted glasses exhibited lower activation energies than these of Sr containing glasses. This may be attributed to the formation of a more disrupted glass network in the case of Ba containing glasses as well as more non-bridging oxygens with the larger cation substitution. It is therefore logical to conclude that in the case of Mg which is a smaller cation compared to Ba, Sr and Ca the change in the activation energy should be different. It is clear from Table 3.4 that between the Kissinger and Marotta methods, the activation energies are in good agreement for all the glasses with nucleation hold confirming the assumption of n=m=3 and consequently bulk nucleation and crystallisation.

CHAPTER 5

CONCLUSIONS

The effect of Mg substitution on the structure of ionomer glasses and glass ceramics was studied by using a combination of analytical methods such as FTIR, DSC and XRD. The optimum nucleation temperature and the activation energy of Ca-FAP/Wagnerite crystallisation was also measured using both the Kissinger and Marotta methods. The Helium Pycnometer was used to measure the density of glasses and glass ceramics.

The density of glasses decreased with increasing the molar content of Mg as expected considering that Mg has a smaller atomic weight and ionic radius than the atomic weight and ionic radius of Ca. Furthermore, the oxygen density increased slightly with Mg substitution most likely due to better packing of atoms in the glass network with Mg substitution for Ca. The density of glass ceramics on the other hand decreased with increasing the molar content of Mg as expected because of the formation of Wagnerite (Wagnerite exhibits lower density than Fluorapatite) that progressively replaces Fluorapatite.

The FTIR spectra showed that there are four absorption regions of Mg containing aluminosilicate glasses, associated with the following:

- Si-O-Si (Q^4) and Si-O-Si (Q^3) stretching vibrations as well as Si-O-[NBO],
- Al-O vibrations with Al in four-fold coordination state,
- P-O bending vibrations and Si-O-Al linkages and Si-O-Si bending vibrations.

The spectra did not show significant changes with Mg substitution other than some shift towards higher wavenumbers with Mg substitution.

DSC analysis showed that the glass transition temperature Tg did not undergo significant changes with Mg substitution but decreased slightly up to 50% Mg substitution and then increased slightly with the progressive substitution of Mg for Ca. This can be explained considering the mixed cation effect. Also, not significant changes were observed for Tp1 and Tp2 comparing all Mg substituted glasses but a significant change was observed between the Tp1 and Tp2 values of LG26 and Mg substituted glasses. Among Mg substituted glasses, the Tp1 and Tp2 values increased or decreased slightly with substitution and often this behaviour has been characterised as the mixed cation effect. The optimum nucleation temperature (Tn) on the other hand decreased as Mg substitution increased. Consequently, a well defined Tn was calculated for all the samples according to the first crystallisation peak temperature except for LG26 100%Mg containing glass which did not exhibit a Tn. It is likely that this glass was phase separated and the crystallisation occured spontaneously without going through the nucleation phase.

XRD analysis showed that the substitution of Mg for Ca resulted in the formation of Wagnerite (Mg_2PO_4F), Ca-FAP and Mullite ($Al_6Si_2O_{13}$) in the case of LG26(25%)Mg and LG26(50%)Mg containing glass ceramics whereas the formation of Wagnerite (Mg_2PO_4F) and Mullite ($Al_6Si_2O_{13}$) was observed in the case of LG26(75%)Mg and LG26(100%)Mg glass ceramics. Furthermore, the crystal size of hexagonal Ca-FAP was calculated to be in the range of 84 to 26 nm, the crystal size of orthorhombic

Mullite was calculated in the range of 31 to 72 nm while the crystal size of monoclinic Wagnerite was in the range of 30 to 42 nm. The Mg substituted glasses which were heat treated up to the first crystallisation temperature Tp1 showed that only Ca-FAP ($Ca_5(PO_4)_3F$) was formed in LG26(25%)Mg glass ceramic whereas Wagnerite (Mg_2PO_4F) was the only phase formed in LG26(75%)Mg glass ceramic.

The activation energy of Ca-FAP/Wagnerite increased for all glass compositions with the exception of LG26(75%)Mg where Wagnerite was the only phase formed at Tp1 and therefore the activation energy was expected to decrease. The activation energies values were in good agreement between the Kissinger and Marotta methods for all the glasses with nucleation hold indicating bulk nucleation and crystallisation as the main crystallisation mechanism.

CHAPTER 6

FUTURE WORK

The following future work can be suggested:

1. The first crystallization temperature corresponds to both Fluorapatite and Wagnerite that crystallize both at the same temperature. It would be interesting to identify what phase is forming first in order to be able to calculate the activation energy of each one crystal phase separately. For this further DSC analysis is required.

2. It would be interesting to measure the degree of crystallisation for all Mg substituted glass ceramics by XRD analysis. Glass-ceramics are polycrystalline materials prepared by the controlled crystallisation of highly viscous glass-forming melts. Their properties depend on the kind and the percentage of crystal phase formed and on the composition of the residual glass. Therefore, the determination of the degree of crystallisation is very important.

3. The study of different substitutions offered a very good insight of the role of cations in the glass network. It is interesting that Ba, Sr and Ca are clearly network modifiers whereas Mg and Zn have been also considered as intermediate oxides (based on other published work). This study offered some useful information on the effect of Mg on the glass structure but there is no evidence about the role of Mg in the glass network. The possibility that under certain conditions Mg can act as a network former is very attractive as this will lead to the formation of Al-free glasses that are very desirable for biomedical applications.

4. Biocompatibility tests should be conducted on all Mg crystallised glasses in order to assess their possibility as bone replacements for medical and dental applications.

REFERENCES

[1] K. Stanton and R. Hill, "The role of fluorine in the devitrification of SiO2·Al2O3·P2O5·CaO·CaF2 glasses," *Journal of Materials Science*, vol. 35, pp. 1911–1916, 2000.

[2] R. Hill, A. Stamboulis, R. V. Law, A. Clifford, M. R. Towler, and C. Crowley, "The influence of strontium substitution in fluorapatite glasses and glass ceramics," *Journal of Non-Crystalline Solids*, vol. 336, pp. 223–229, 2004.

[3] R. G. Hill, A. Stamboulis, and R. V. Law, "Characterisation of fluorine containing glasses by F-19, Al-27, Si-29 and P-31 MAS-NMR spectroscopy," *Journal of Dentistry*, vol. 34, pp. 525–532, 2006.

[4] A. Moshaverinia, N. Roohpour, Ihtesham U. Rehman, "Synthesis and characterisation of a novel fast-set proline-derivative-containing glass ionomer cement with enhanced mechanical properties," *Acta Biomaterials*, vol. 5, pp. 498-507, 2009.

[5] J. W. Nicholson, "Chemistry of glass-ionomer cements: a review," *Biomaterials*, vol. 19, pp. 485–494, 1998.

[6] C. Fernandez, J. P. Amoureux, "2D multiquantum MAS-NMR spectroscopy of 27Al in aluminophosphate molecular sieves," *Chemical Physics Letters*, vol. 242, pp. 449-454, 1995.

[7] S. G. Griffin and R. G. Hill, "Influence of glass composition on the properties of glass polyalkenoate cements. Part IV: influence of fluorine content," *Biomaterials*, vol. 2, pp. 693–698, 2000.

[8] Carel L. Davidson, Ivar A. Mjor: Glass-Ionomer Cements, 1999.

[9] Graham J Mount: An atlas of Glass Ionomer Cements, 1990.

[10] C. M Crowley, J. Doyle, M. R. Towler, R. G Hill, S. Hampshire, "The influence of capsule geometry and cement formulation on the apparent viscosity of dental cement," *Journal of dentistry*, vol. 34, pp. 566-573, 2006.

[11] Artemis Stamboulis, Fei Wang, "Ionomer glasses: Design and Characterisation," in "*Advanced Biomaterials*", ed. B. Basu, D.S. Katti, A.Kumar, John Wiley & Sons, 2009, pp.411-433.

[12] Alan D. Wilson/John W. McLean: Glass-Ionomer Cement, 1988.

[13] A. Guida, R. G. Hill, M. R. Towler, S. Eramo, "Fluoride release of model glass ionomer cements", *Journal of materials science: Materials in Medicine* vol. 13, pp. 645-649, 2002.

[14] D.Boyd, H. Li and D. A. Tanner, "The antibacterial effect of zinc ion migration from zinc-based glass polyalkenoate cements," *Springer Science,* vol.17, pp. 489-494, 2006.

[15] R. Hill and D. Wood, "Apatite-mullite glass ceramics," *Journal of Materials Science*, vol. 6, pp. 311–318, 1995.

[16] A. Rafferty, A. Clifford, R. Hill, D. Wood, B. Samuneva, and M. Dimitrova-Lukacs, "Influence of fluorine content in apatite-mullite glass ceramics," *Journal of the American Ceramic Society*, vol. 83, pp. 2833–2838, 2000.

[17] S. Griffin, R. G Hill, "Glass composition influence on glass polyalkenoate cement mechanical properties," *Journal of non-crystalline solids,* vol.196, pp. 255-259, 1996.

[18] C. M. Gorman and R. G. Hill, "Heat-pressed ionomer glass-ceramics. Part I: an investigation of flow microstructure", *Dental Materials*, vol.19, pp. 320-326, 2003.

[19] Arun K. Varshneya: fundamentals of Inorganic Glasses, 2006

[20] A. Calver, R. G. Hill, and A. Stamboulis, "Influence of fluorine content on the crystallization behavior of apatite-wollastonite glass ceramics," Journal of Materials Science, vol. 39, pp. 2601-2603, 2004.

[21] R. D. Goodridge, D. J. Wood, C. Ohtsuki, and K. W. Dalgarno, "Biological evaluation of an apatite-mullite glass-ceramic produced via selective laser sintering," *Acta Biomaterialia*, vol. 3, pp. 221-231, 2007.

[22] A. D. Neve, V. Piddock, and E. C. Combe, "The effect of glass heat treatment on the properties of a novel polyalkenoate cement," *Clinical Materials*, vol. 12, pp. 113, 1993.

[23] D. Boyd, M. R. Towler, R. V. Law, and R. G. Hill, "An investigation into the structure and reactivity of calcium-zinc-silicate ionomer glasses using MAS-NMR spectroscopy," *Journal of Materials Science: Materials in Medicine*, vol. 17, 2006.

[24] C. O. Freeman, I. M. Brook, A. Johnson, P. V. Hatton, R. G. Hill, and K. T. Stanton, "Crystallization modifies osteoconductivity in an apatite–mullite glass–ceramic," *Journal of Materials Science: Materials in Medicine*, vol. 14, pp. 985-990, 2003.

[25] S. G. Griffin and R. G. Hill, "Influence of glass composition on the properties of glass polyalkenoate cements. Part I: influence of aluminium to silicon ratio," *Biomaterials*, vol. 20, pp. 1579–1586, 1999.

[26] S. G. Griffin and R. G. Hill, "Influence of glass composition on the properties of glass polyalkenoate cements. Part II: influence of phosphate content," *Biomaterials*, vol. 21, pp. 399–403, 2000.

[27] A. Rafferty, R. Hill, and D. Wood, "Amorphous phase separation of ionomer glasses,"*Journal of Materials Science*, vol. 35, pp. 3863–3869, 2000.

[28] A. D. Wilson, S. Crisp, H. J. Prosser, B. G. Lewis, and S. A. Merson, "Aluminosilicate Glasses For Poly-Electrolyte Cements," *Industrial & Engineering Chemistry Product Research And Development*, vol. 19, pp. 263-270, 1980.

[29] R. G. Hill and A. D. Wilson, "Some structural aspects of glasses used in ionomer cements," *Glass Technology*, vol. 29, pp. 150-157, 1988.

[30] Q. Zeng and J. F. Stebbins, "Fluoride sites in aluminosilicate glasses: High-resolution F-19 NMR results," *American Mineralogist*, vol. 85, pp. 863-867, 2000.

[31] E. De Barra and R. G. Hill, "Influence of glass composition on the properties of glass polyalkenoate cements. Part III: influence of fluorite content," *Biomaterials*, vol. 21,pp. 563–569, 2000.

[32] A. Guida, R. G. Hill, M. R. Towler, S. Eramo, "Fluoride release of model glass ionomer cements," *Journal of materials science: Materials in Medicine* vol. 13, pp. 645-649, 2002.

[33] A. Stamboulis, R. G. Hill, and R. V. Law, "Characterisation of the structure of calcium alumino-silicate and calcium fluoro-alumino-silicate glasses by magic angle spinning nuclear magnetic resonance (MAS-NMR)," *Journal of Non-Crystalline Solids*, vol.333, pp. 101–107, 2004.

[34] R. G. Hill, A. Stamboulis, and R. V. Law, "Characterisation of fluorine containing glasses by F-19, Al-27, Si-29 and P-31 MAS-NMR spectroscopy," *Journal of Dentistry*, vol. 34, pp. 525–532, 2006.

[35] A. Stamboulis, R. G. Hill, and R. V. Law, "Characterisation of the structure of calcium alumino-silicate and calcium fluoro-alumino-silicate glasses by magic angle spinning nuclear magnetic resonance (MAS-NMR)," *Journal of Non-Crystalline Solids*, vol. 333, pp. 101-107, 2004.

[36] A. Stamboulis, R. G. Hill, and R. V. Law, "Structural characterization of fluorine containing glasses by F-19 Al-27 Si-29 and P-31 MAS-NMR spectroscopy," *Journal of Non-Crystalline Solids*, vol. 351, pp. 3289-3295, 2005.

[37] J. F. Stebbins, S. Kroeker, S. K. Lee, and T. J. Kiczenski, "Quantification of five- and six-coordinated aluminum ions in aluminosilicate and fluoride-containing glasses by high-field, high-resolution Al-27 NMR," *Journal of Non-Crystalline Solids*, vol. 275, pp. 1-6, 2000.

[38] F. Wang, PhD Thesis, "Cation Substitution in ionomer glasses: Effect on glass structure and crystallisation," University of Birmingham, 2009.

[39] R. Hill, A. Calver, A. Stamboulis, and N. Bubb, "Real time nucleation and crystallisation studies of a fluorapatite glass-ceramics using small angle neutron scattering and neutron diffraction," *Journal of the American Ceramic Society*, vol. 90, pp. 763-768, 2007.

[40] A. Clifford, A. Rafferty, R. Hill, P. Mooney, D. Wood, B. Samuneva, and S. Matsuya, "The influence of calcium to phosphate ratio on the nucleation and crystallisation of apatite glass-ceramics," *Journal of Materials Science: Materials in Medicine*, vol. 12, pp. 461-469, 2001.

[41] F. C. M. Driessens and R. M. H. Veerbeck, *Biominerals*: CRC, 1990.

[42] F. Wang, A. Stamboulis, D. Holland, S. Matsuya, and A. Takeuchi, "Solid state MAS NMR and FTIR study of barium containing aluminosilicate glasses, " *Key Engineering Materials*, vol. 361–363, pp. 825–828, 2008.

[43] M. Darling and R. Hill, "Novel polyalkenoate (glass-ionomer) dental cements based on zinc silicate glasses," *Biomaterials*, vol. 15, pp. 299-306, 1994.

[44] S. Watts, Phd Thesis, "Composition structure property relationships in bioactive glasses," Imperial College of London, 2010.

[45] W. Lowenstein, "The distribution of aluminium in the tetrahedral of silicates and aluminates," *American Mineralogist*, vol. 39, pp. 92-96, 1954.

[46] A. Clifford, A. Rafferty, R. Hill, P. Mooney, D. Wood, B. Samuneva, and S. Matsuya, "The influence of calcium to phosphate ratio on the nucleation and crystallisation of apatite glass-ceramics," *Journal of Materials Science: Materials in Medicine*, vol. 12, pp. 461-469, 2001.

[47] R. Hill, D. Wood, and M. Thomas, "Trimethylsilylation analysis of the silicate structure of fluoro-alumino-silicate glasses and the structural role of fluorine," *Journal of Materials Science*, vol. 34, pp. 1767-1774, 1999.

[48] A. L. Patterson, "The Scherrer formula for x-ray particle size determination," *Physical Review*, vol. 56, pp. 978-982, 1939.

[49] A. Weibel, R. Bouchet, F. Boulc'h, and P. Knauth, "The big problem of small particles: A comparison of methods for determination of particle size in nanocrystalline anatase powders," *Chemistry of Materials*, vol. 17, pp. 2378-2385, 2005.

[50] J. E. Shelby, "Introduction to Glass Science and Technology (RSC paperbacks)," The Royal Society of Chemistry, 1997.

[51] T. I. Barry, D. J. Clinton, and A. D. Wilson, "The structure of a glass-ionomer cement and its relationship to the setting process," *Journal of Dental Research*, vol. 58, pp. 1072-1079, 1979.

[52] M. J. Davis and I. Mitra, "Crystallization measurements using DTA methods: Applications to Zerodur," *Journal of The American Ceramic Society*, vol. 86, pp. 1540-1546, 2003.

[53] D.Wood and R.Hill, "Structure-Property Relationships in Ionomer Glasses," *Clinical Materilas*, vol.7, pp. 301-312, 1991.

[54] Kazuma Matusita and Sumio Sakka, "Kinetic study on crystallization of glass by Differential Thermal Analysis- Criterion on application of Kissinger plot, " *Journal of Non-Crystalline Solids,* vol. 38, pp. 741-746, 1980.

[55] P. Islam, R. Hill, A. Stamboulis, "Activation Energy for crystal growth in stoichiometric $CaAl_2Si_2O_9$ glasses, " *Journal of Materials Science Letters,* vol.22, pp.1287-1289, 2003.

[56] L. Stoch and M. Sroda, "Infrared spectroscopy in the investigation of oxide glasses structure," *Journal of Molecular Structure*, vol. 512, pp. 77-84, 1999.

[57] S. A. MacDonald, C. R. Schardt, D. J. Masiello, and J. H. Simmons, "Dispersion analysis of FTIR reflection measurements in silicate glasses," *Journal of Non-Crystalline Solids*, vol. 275, pp. 72-82, 2000.

[58] C. Huang and E. C. Behrman, "Structure And Properties Of Calcium Aluminosilicate Glasses," *Journal of Non-Crystalline Solids*, vol. 128, pp. 310-321, 1991.

[59] L. G. Hwa, S. L. Hwang, and L. C. Liu, "Infrared and Raman spectra of calcium alumino-silicate glasses," *Journal of Non-Crystalline Solids*, vol. 238, pp. 193-197, 1998.

[60] O. Peitl, E. D. Zanotto, and L. L. Hench, "Highly bioactive P_2O_5-Na_2O-CaO-SiO_2 glass-ceramics," *Journal of Non-Crystalline Solids*, vol. 292, pp. 115-126, 2001.

[61] A. Chowdhuri, D.-U. Jin, J. Rosado, and C. Takoudis, "Strain and substoichiometry at the $Si(100)/SiO_2$ interface," *Physical Review B*, vol. 67, pp. 245305, 2003.

[62] A. E. Geissberger and F. L. Galeener, "Raman studies of vitreous SiO_2 versus fictive temperature," *Physical Review B*, vol. 28, pp. 3266-3271, 1983.

[63] P. N. Sen and M. F. Thorpe, "Phonons in Ax_2 glasses - from molecular to band-like modes," *Physical Review B*, vol. 15, pp. 4030-4038, 1977.

[64] J. Serra, P. Gonzalez, S. Liste, C. Serra, S. Chiussi, B. Leon, M. Perez-Amor, H. O. Ylanen, and M. Hupa, "FTIR and XPS studies of bioactive silica based glasses," *Journal of Non-Crystalline Solids*, vol. 332, pp. 20-27, 2003.

[65] N. J. Clayden, S. Esposito, A. Aronne, and P. Pernice, "Solid state Al-27 NMR and FTIR study of lanthanum aluminosilicate glasses," *Journal of Non-Crystalline Solids*, vol. 258, pp. 11-19, 1999.

[66] N. Srinivasa Rao, S. Bale, M. Purnima, K. Siva Kumar, and S. Rahman, "Mixed alkali effect in boroarsenate glasses," *Journal of Physics and Chemistry of Solids*, vol. 68, pp. 1354-1358, 2007.

[67] H. Jain, N. L. Peterson, and H. L. Downing, "Tracer diffusion and electrical-conductivity in sodium cesium silicate-glasses," *Journal of Non-Crystalline Solids*, vol. 55, pp. 283-300, 1983.

[68] B. Z. Pevzner and V. P. Klyuev, "Manifestation of the mixed-cation effect in dilatometric properties of RO (R_2O) center dot 2B(2)O(3) borate glasses upon replacement of Na_2O by BaO, Na_2O by MgO, and BaO by MgO," *Glass Physics And Chemistry*, vol. 30, pp. 506-514, 2004.

[69] A. Weibel, R. Bouchet, F. Boulc'h, and P. Knauth, "The big problem of small particles: A comparison of methods for determination of particle size in nanocrystalline anatase powders," *Chemistry of Materials*, vol. 17, pp. 2378-2385, 2005.

[70] H. Eshtiagh-Hosseini, M. R. Housaindokht, and M. Chahkandi, "Effects of parameters of sol-gel process on the phase evolution of sol-gel-derived hydroxyapatite," *Materials Chemistry and Physics*, vol. 106, pp. 310-316, 2007.